ORIGINAL RESEARCH

Role of Inflammation in the Development of COVID-19 to Parkinson's Disease

Tingting Liu[1],*, Haojie Wu[1],*, Lin Sun[2], Jianshe Wei[1]

[1]Institute for Brain Sciences Research, School of Life Sciences, Henan University, Institute of Neurourology and Urodynamics, Huaihe Hospital of Henan University, Kaifeng, 475004, People's Republic of China; [2]College of Chemistry and Molecular Sciences, Henan University, Kaifeng, 475004, People's Republic of China

*These authors contributed equally to this work

Correspondence: Lin Sun; Jianshe Wei, Email sunlin@vip.henu.edu.cn; jswei@henu.edu.cn

Background: The coronavirus disease 2019 (COVID-19) can lead to neurological symptoms such as headaches, confusion, seizures, hearing loss, and loss of smell. The link between COVID-19 and Parkinson's disease (PD) is being investigated, but more research is needed for a definitive connection.

Methods: Datasets GSE22491 and GSE164805 were selected to screen differentially expressed gene (DEG), and immune infiltration and gene set enrichment analysis (GSEA) of the DEG were performed. WGCNA analyzed the DEG and selected the intersection genes. Potential biological functions and signaling pathways were determined, and diagnostic genes were further screened using gene expression and receiver operating characteristic (ROC) curves. Screening and molecular docking of ibuprofen as a therapeutic target. The effectiveness of ibuprofen was verified by constructing a PD model in vitro, and constructing "COVID19-PD" signaling pathway, and exploring the role of angiotensin-converting enzyme 2 (ACE2) in PD.

Results: A total of 13 DEG were screened from the GSE36980 and GSE5281 datasets. Kyoto encyclopedia of genes and genomes (KEGG) analysis showed that the DEG were mainly associated with the hypoxia-inducible factor (HIF-1), epidermal growth factor receptor (EGFR) tyrosine kinase inhibitor resistance, etc. After analysis, it is found that ibuprofen alleviates PD symptoms by inhibiting the expression of nuclear factor kappa-B (NF-κB), interleukin-1β (IL-1β), IL-6, and tumor necrosis factor-α (TNF-α). Based on signal pathway construction, the importance of ACE2 in COVID-19-induced PD has been identified. ACE2 is found to have widespread distribution in the brain. In the 1-methyl-4-phenyl-1,2,3,6-te-trahydropyridine (MPTP)-induced *ACE2*-null PD mice model, more severe motor and non-motor symptoms, increased NF-κB p65 and α-synuclein (α-syn) expression with significant aggregation, decreased tyrosine hydroxylase (TH), severe neuronal loss, and neurodegenerative disorders.

Conclusion: Severe acute respiratory syndrome coronavirus 2 (SARS-CoV-2) infection increases the risk of PD through an inflammatory environment and downregulation of ACE2, providing evidence for the molecular mechanism and targeted therapy associated with COVID-19 and PD.

Keywords: Parkinson's disease, COVID-19, ibuprofen, nuclear factor kappa-B, angiotensin-converting enzyme 2

Introduction

Coronavirus disease 2019 (COVID-19) was initially identified in December 2019 in the city of Wuhan, China. Since then, it has rapidly spread across the globe, causing significant loss of human lives and severe economic consequences. The world has recorded over 760 million cases and 6.9 million deaths, but the actual number is considered higher. Common symptoms of COVID-19 infection include coughing, fever, and difficulty breathing. Additionally, there have been increasing reports of muscle pain, loss of smell (anosmia) or reduced ability to smell (hyposmia), and loss of taste.[1] Recent reports indicate that the SARS-CoV-2 virus, responsible for COVID-19 infection, may invade the central nervous system (CNS), leading to potential long-term complications. These complications can often go unnoticed for an extended period of time. Evidence suggests that the virus can enter the CNS through various routes, including the angiotensin-converting enzyme 2 (ACE2) receptor, neuronal transport, haematogenous route, and nasal route via the olfactory bulb

3259

and cribriform plate. It can then propagate through trans-synaptic signaling and exhibit retrograde movement along nerve fibers.[2–4] The SARS-CoV-2 virus enters host cells by attaching its viral spike protein to the ACE2 receptor, which is present on various mammalian cells. This attachment is facilitated by the serine protease transmembrane protease serine 2 (TMPRSS2), which primes the spike protein.[5] Both ACE2 and TMPRSS2 have been detected on ciliated epithelial cells and oligodendrocytes, suggesting a potential route for CNS penetration.[6] The virus can also infect endothelial cells, which express ACE2 throughout the body, including within the brain. This allows the virus to travel across capillaries and enter glial cells within the CNS through vesicles.[7] COVID-19 infection can induce inflammation and neurological damage in the CNS through various mechanisms, including damage to the ACE2 receptor, cytokine-related injury or cytokine storm syndrome, secondary hypoxia, demyelination, disruption of the blood-brain barrier (BBB), neurodegeneration, neuroinflammation, oxidative stress, and mitochondrial dysfunction. Reports have associated viral invasion into the CNS with complications such as Parkinson's disease (PD), Alzheimer's disease (AD), meningitis, encephalopathy, anosmia, hyposmia, anxiety, depression, psychiatric symptoms, seizures, stroke, etc.[8–10]

The use of non-steroidal anti-inflammatory drugs (NSAIDs) such as ibuprofen for COVID-19 treatment has been a topic of interest. Ibuprofen is a widely used and safe NSAID recommended for relieving pain and inflammation in patients, including those with COVID-19.[11,12] However, the exact molecular mechanism underlying the anti-inflammatory effects of ibuprofen remains unclear, and further research is needed in this area. It is known that nuclear transcription factor-kappa B (NF-κB), present in the cytoplasm of cells, plays a role in the transcription of genes associated with inflammation when activated.[13,14] NF-κB p65 can be activated by SARS-CoV-2 through the activation of pattern recognition receptors (PRRs).[15,16] In vitro studies have shown that ibuprofen can suppress NF-κB p65 activity, thereby reducing inflammation in COVID-19 patients.[17] Patients with PD have a higher susceptibility to COVID-19 infection due to their advanced age.[18] The theory of inflammation has gained substantial support due to the similarities between the inflammatory pathways involved in COVID-19 and the ones potentially responsible for Parkinson's development.[19,20] Pro-inflammatory cytokines such as tumor necrosis factor alpha (TNF-α) and interleukin-1β (IL-1β) have been linked to an increased risk of PD, while the use of anti-TNF biologics may lower this risk.[21] Furthermore, oxidative stress and NF-κB are also suspected to contribute to the onset of both COVID-19 and PD.[22] Therefore, it has been proposed that ibuprofen could be used to manage PD in the context of COVID-19, as both diseases involve inflammatory processes.

The brain renin-angiotensin system (RAS) has a significant impact on autonomic and neuroendocrine functions, as well as cardiovascular homeostasis. Angiotensin-II (Ang-II) is the primary effector molecule in RAS and exerts most of its physiological functions, including the regulation of blood pressure, through activation of angiotensin type-1 (AT1) receptors.[23,24] When the brain RAS is dysregulated, increased synthesis of Ang-II leads to sympathetic outflow and hypertension. Two decades ago, brain ACE2 was discovered as a component of RAS that counteracts the adverse cardiovascular effects of Ang-II. Recent studies have shown that ACE2 also plays critical roles in neuro-inflammation, gut dysbiosis, and the regulation of stress and anxiety-like behaviors.[23] Identification of brain ACE2-expressing neurons in rats and their functional circuits can help predict potential neurological manifestations resulting from dysregulation of ACE2 during and after COVID-19 infection.[25] PD is the second most common neurodegenerative disorder, affecting around 2% of individuals over the age of 60.[26] PD is characterized by motor symptoms like resting tremor, rigidity, and bradykinesia, as well as non-motor symptoms such as psychosis, depression, hyposmia, autonomic dysfunction, and cognitive impairment.[26,27] COVID-19 has been associated with significant decline in both motor and non-motor performance in PD patients.[28] Advanced age and longer duration of PD may increase the susceptibility to SARS-CoV-2 infection.[29] Growing evidence suggests that ACE2 plays a crucial role in the pathogenesis of both COVID-19 and PD, as it is involved in common underlying mechanisms such as inflammation, immune response, oxidative stress, cell proliferation and survival, and mitochondrial function. Although the role of ACE2 in neurodegenerative diseases and COVID-19 has been previously discussed,[30,31] its role in PD has not been studied. Given the rapid growth of research on the interaction between neurodegenerative diseases and COVID-19, we used the GEO dataset to analyze the biological functions and diagnostic value of the hub genes of the two diseases, as well as the therapeutic effects of ibuprofen on PD cell models. At the same time, we constructed the signaling pathways of PD and COVID-19 and found that ACE2 plays an important role in both diseases. Therefore, we used mice with *ACE2*-null to induce PD animal models to elucidate the role of ACE2 in PD pathology, providing insights for future research and the development of ACE2 related targeted therapy methods.

Methods

Data Acquisition

The mRNA announcement contour databases, GSE22491, GSE164805, GSE49036, GSE171110, GSE153970, and GSE175779, were downloaded from the gene expression omnibus (GEO) database (https://www.ncbi.nlm.nih.gov/).[32] Clinical characteristics of samples from GSE22491 and GSE164805 datasets was shown in Supplementary Tables S1 and S2. The dataset information are listed in Table 1. Quality control and normalization of the gene expression profiles were carried out using the scale function in the R package 4.2.0 software. Boxplots were used to represent the normalized data. Principal component analysis (PCA) was utilized to confirm the consistency of the data, while the PCA plots were generated using the R package ggord. The experimental flowchart for this study is shown in Figure 1.

Immune Infiltration and GSEA

A violin plot was used to depict the differential expression levels of differentially expressed gene (DEG) between PD patients and healthy controls. For immune infiltration analysis, we employed the single-sample gene set enrichment analysis (ssGSEA) algorithm provided in the R package-GSVA.[33] To prepare gene expression data for this analysis, a gene expression matrix was constructed where genes were represented in rows and samples in columns. Immune-related gene sets containing genes associated with immune cell types or immune functions were downloaded. A predefined set of 24 markers for immune cells from reference[33] was utilized to calculate immune infiltration in the uploaded data. To perform the ssGSEA analysis, we used the gsva(data) function from the GSVA package, inputting the gene expression data and immune-related gene sets. Heatmaps and boxplots were employed to visualize the expression levels of immune cells in PD and COVID-19 patients compared to healthy controls. Furthermore, Gene Set Enrichment Analysis (GSEA) was conducted using the GSEA software (version 4.1.0)[34] to explore potential underlying mechanisms in PD and COVID-19. Start with gene expression data, typically represented as a matrix. Choose a specific gene set collection that you want to analyze. Rank the genes in your dataset based on differential expression genes. Perform GSEA package and examine the GSEA results to identify gene sets that are significantly enriched in the high or low end of the ranked gene list. Pay attention to the normalized enrichment score (NES), which quantifies the enrichment level of each gene set. Investigate the biological functions and pathways. DEG were identified based on a significance threshold of *P-value*<0.05, and enriched pathways identified through GSEA were filtered using a *P-value*<0.05.

Table 1 The Detailed Information of the Datasets

| Dataset	Database	Data type	Platform	Information
GSE22491	GEO	RNA-seq	GPL6480 Agilent-014850 Whole Human Genome Microarray 4x44K G4112F	10 PD patients and 8 healthy controls from peripheral mononuclear blood cells (PBMCs)
GSE164805	GEO	RNA-seq	GPL26963 Agilent-085982 Arraystar human lncRNA V5 microarray	10 COVID-19 patients and 5 healthy controls from PBMCs
GSE49036	GEO	RNA-seq	GPL570 [HG-U133_Plus_2] Affymetrix Human Genome U133 Plus 2.0 Array	Control Braak α- synuclein Stage 0: 8 samples; α Braak α-synuclein stage 1–2: 5 samples; Braak α-synuclein 3–4 7 samples; Braak α-synuclein stages 5–6: 8 samples from substantia nigra
GSE171110	GEO	RNA-seq	GPL16791 Illumina HiSeq 2500 (Homo sapiens)	44 patients with COVID-19 and 10 healthy people from whole blood gene expression profiles
GSE153970	GEO	RNA-seq	GPL24676 Illumina NovaSeq 6000 (Homo sapiens)	pHAE cultures were infected apically with SARS-CoV-2 (MOI= 0.25) for 48 hours, at which point mock and SARS-CoV-2 infected (n=3) samples
GSE175779	GEO	RNA-seq	GPL18573 Illumina NextSeq 500 (Homo sapiens)	Primary human bronchial epithelial cells (HBECs) from normal, nonsmoker, aged individuals (>67 years old) either uninfected or infected with SARS-CoV-2 as a function of time post-infection (24, 48, 72 and 96 hr)
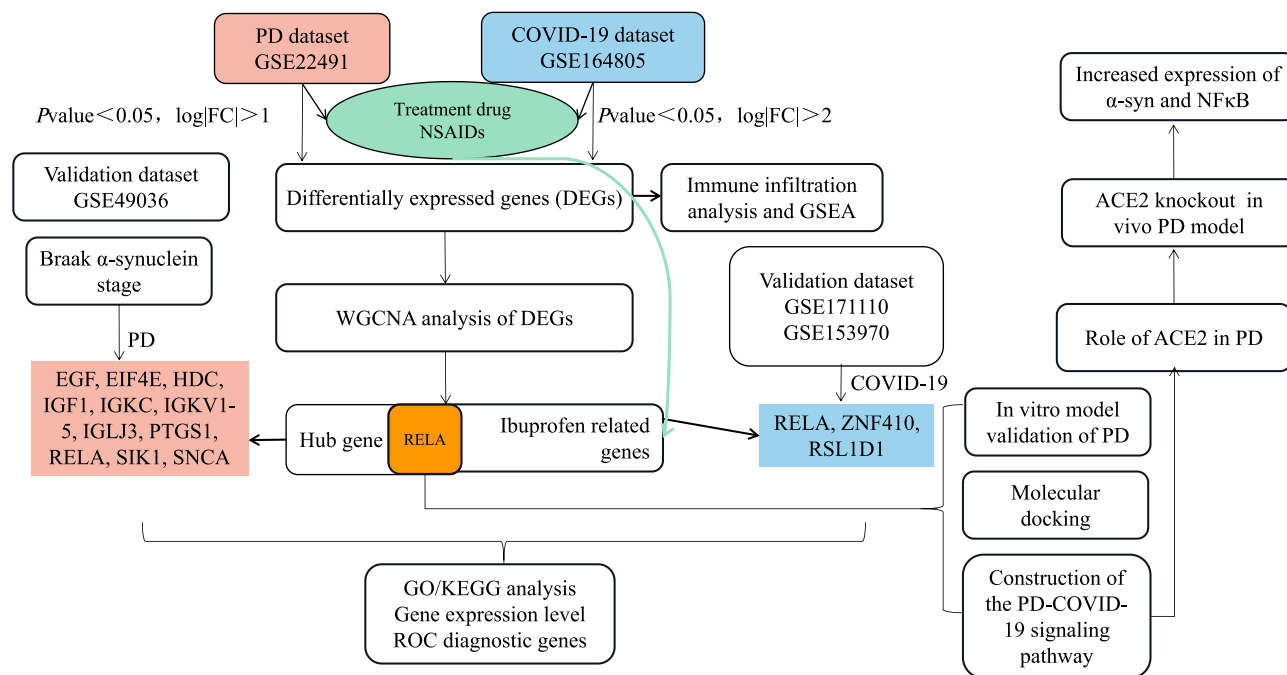
Figure 1 The flow chart of this study.

WGCNA Identification of DEG

The objective of WGCNA is to identify modules of co-expressed genes and investigate the relationship between gene networks and phenotypes of interest, as well as identify hub genes within these networks. To achieve this, we construct a weighted adjacency matrix that emphasizes strong gene relationships and penalizes weak correlations. The adjacency matrix is then transformed into a topological overlap matrix (TOM), which quantifies the connectivity of genes in the network. The TOM measures the connectivity of neighboring genes and computes dissimilarity. To group genes with similar expression profiles, we employed average linkage hierarchical clustering based on the dissimilarity estimated by the TOM. The resulting gene modules are visually represented by branches and different colors in the cluster tree, aiding in the identification of module relationships and relevant genes.[35]

Identification of Diagnostic Genes

The "venneuler" package in R 4.2.0 software was adopted to draw the intersection of PD or COVID-19 and ibuprofen, and a total of 556 targets of ibuprofen from the comparative toxicogenomics database (CTD) (https://ctdbase.org/) were cross-referenced between PD and COVID-19 patients. The analysis of Kyoto encyclopedia of genes and genomes (KEGG) pathway and Gene Ontology (GO) enrichment for the DEG was conducted using the "clusterProfiler" and "GOplot" packages in R software. To identify diagnostic genes, ROC curve analysis was performed, and the results were visually displayed. The area under the curve (AUC) was calculated using the pROC package in R software to determine the predictive values of the hub genes.[36] Diagnostic genes were selected from the set based on the criterion of an AUC > 0.700.

Molecular Docking

To investigate how drug candidates interact and bind to their targets, we used AutodockVina 1.2.2, software to simulate the docking of proteins and ligands.[37] Molecular structures were obtained from PubChem (https://pubchem.ncbi.nlm.nih.gov/).[38] The 3D structures of RELA (PDB ID: 6QHL) and NF-κB (PDB ID: 1NFK) were downloaded from the Protein Data Bank (PDB) (http://www.rcsb.org/pdb/). All protein and molecular files were converted to PDBQT format for the purpose of docking analysis, which involved excluding water molecules and adding polar hydrogen atoms. A grid box was positioned to encompass the domain of each protein and allow for molecular movement. The dimensions of the grid box were set as $30 \times 30 \times 30$ Å with a grid point distance of 0.05 nm. Autodock Vina 1.2.2 (http://autodock.scripps.edu/),

was employed for the molecular docking studies. The COVID and PD pathway networks were constructed by integrating pathways from the KEGG database (https://www.genome.jp/kegg/). Additionally, the expression of the *ACE2* gene in various brain cells was analyzed using the Human Transcriptome Cell Atlas database (https://www.htcatlas.org/).

In vitro Experiment Verification
Cell Culture
The SH-SY5Y dopaminergic neuronal cell line was purchased from Servicebio (China, Wuhan). The cells were cultured in high-glucose Dulbecco's modified Eagle's medium (DMEM) (Gibco Laboratories, Grand Island, NY, USA), supplemented with 10% fetal bovine serum, penicillin (100 units/mL), and streptomycin. The cells were incubated at 37 °C in a humidified atmosphere with 5% CO_2. The culture medium was refreshed every 2–3 days. To induce PD in the in vitro cell models, SH-SY5Y cells were treated with 1 mmol/L MPP^+ (M10041; Abmole, USA) for 24 h. The cells were then used for subsequent experiments. The experimental groups were as follows: control group (SH-SY5Y cells), PD group (SH-SY5Y cells treated with 1 mmol/L MPP^+),[39] ibuprofen (HY-78131, MCE, USA) group (SH-SY5Y cells pretreated with 500 μmol/L ibuprofen),[40] and PD+ibuprofen group (SH-SY5Y cells pretreated with ibuprofen for 24 h and then incubated with 1 mmol/L MPP^+ for 24 h). After treatment, the cells were harvested for Western blotting or immunofluorescence analysis.

In vivo Experiment Verification
Animal
Experiments were carried out using male C57BL/6J mice aged 6–8 weeks and weighing 25–30g, provided by Cyagen Biosciences. Once the transgenic mice of the F0 generation reached sexual maturity at eight weeks, they were bred with wild-type mice, and the resulting F1 generation mice were used for subsequent experiments. The animals were kept under standardized conditions (12/12h light/dark cycle, 22±2 °C, and relative humidity of 55±5%), they had continuous access to food and water. All procedures involving animals were conducted in accordance with the Guide for the Care and Use of Laboratory Animals and were approved by the Institutional Animal Care and Use Committee of Henan University. The experimenters were unaware of the groups to which the mice were assigned. Before the experiment, the animals were given two weeks to acclimate to the facilities. They were then randomly divided into four groups, each consisting of eight mice: the saline group, the PD model group, the *ACE2*-null group, and the *ACE2*-null+1-methyl-4-phenyl-1,2,3,6-tetrahydropyridine (MPTP) group (MPTP, 20 mg/kg/d,[41] the saline group was injected with an equal volume of NaCl and injected intraperitoneally for 15 days). On day 16, at 3 PM, behavioral tests were conducted on all groups of animals. On day 17, at 10 AM, four mice from each group were perfused with 0.9% saline, followed by fixation with 4% paraformaldehyde (PFA), and their brains were collected. Additionally, in each group, four animals had tissues from the substantia nigra (SN) and striatum rapidly dissected on ice, frozen in liquid nitrogen, and stored at −80 °C until further use.

Behavioral Tests

Gait Test. A gray acrylic board with a runway and thickness of 3 mm was used as the testing setup. 200 cm long, 20 cm broad, and 12 cm high make up the runway. During the initial training day, the mice were given time to familiarize themselves with the surroundings. Subsequently, the forepaws were colored red and the hindpaws were colored blue using safe, non-toxic food dyes. Throughout the training session, the mice were trained to run towards the goal box. The stride length was measured by analyzing the average distance between each forepaw and hind paw footprint. A minimum of six values from each experiment were recorded for each parameter.

Rotarod Test. At the start of each experiment, the mice were placed in individual lanes, isolated from one another. The initial velocity of the apparatus was set to 4 rpm. After 300 seconds, the first acceleration to 40 rpm was applied and maintained for an additional 300 seconds.[42] The recorded measurement in each experiment was the average duration, in seconds, that the mice were able to stay on the rod.

Tail Suspension Test. The tail suspension test was utilized to assess depressive behaviors in animals. This method relies on the observation that mice, when suspended by their tails, display immobilization, which can be interpreted as

a reflection of despair or hopelessness. The mice were suspended by their tails using tape on a platform positioned 50 cm above the ground. Immobility was defined as the absence of physical movement while passively suspended, and both limb and body movements were recorded for a duration of 5 min.[43]

Forced Swimming. The forced swimming test was carried out in mice individually forced to swim in an open cylindrical container (diameter 10 cm, height 25 cm), containing 19 cm of water at 25+1°C. In the test session lasting 5 min, an increase in the immobility duration was considered indicative of an increased depression-related behavior.[44]

Open-Field Test. The device used for the test was based on a square field (50×50×30 cm). A lamp positioned 150 cm above the enclosure provided illumination of approximately 100 lx in the central area. For each experiment, the mice were initially placed in a 15×15 cm central area.[45] Various parameters, including the distance traveled, movement speed, and time spent in the central area, were recorded within 5 min interval.

Elevated Plus Maze Test. The experimental apparatus was set up at a height of 50 cm above the ground and consisted of two opposing open arms (50×10 cm), closed arms (50×10×35 cm), and a central zone (10×10 cm). The mice were positioned on a central platform, facing one open arm, while another arm was left free to move for a duration of 5 min. The amount of time spent by the mice in both the open and closed arms was recorded, and the ratio of the time spent in the open arms to the total time was analyzed.

PCR. Tail DNA extraction and amplification were performed in accordance with the manufacturer's instructions. The PCR Primers1 (561bp): F1: 5 '-GACGTTGTGCATTGACTGTTCTA-3', R1: 5 '-CTACATTACCAGGCAAATGGAAGT-3', the PCR Primers 2 (560bp): F1: 5'-GACGTTGTGCATTGACTGTTCTA-3' R2: 5'-TACTTTGCTGAGGGTCAAGGTTTA-3', at 94 °C for 5 min; 33 cycles at 94°C for 30s; 58°C for 30s; 72°C, 25s; the temperature was cooled to 72 °C for 3 min and stored at 4 °C. ACE2 expression was detected using agarose gel electrophoresis. Primer 1 and primer 2 both have bands for heterozygous *ACE2*-null. Only primer 1 has a band for pure *ACE2*-null, while only primer 2 has a band for the wild type (WT).

Analysis of Immunofluorescence and Immunohistochemistry

SH-SY5Y cells ($4×10^5$/mL) were placed on bottle slides. After treatment, the bottle slides were placed in phosphate buffer saline (PBS) and anchored with 4% formaldehyde at an allowed temperature for 30 min. SH-SY5Y cells on the bottle slides were then permeabilized with 0.1% Triton X-100 for 10 min, washed three times with PBS, NF-κB (1:200, affinity) antibodies were incubated overnight in 10% goat serum. After three washes, incubate SH-SY5Y cells with fluorescent secondary antibody (1:2000, Invitrogen) for 2 h, and then stain the nucleus with DAPI for 10 min. Immunohistochemistry and immunofluorescence was performed on 30 μm thick serial brain sections., We used 1xCitrate Antigen Retrieval Solution, 98 °C for 10 min, 0.1% Triton X−100 transparent for 10 min, hydrogen peroxide for 20 min (dark), and blocked with 10% goat serum in PBS incubated with tyrosine hydroxylase (TH) (1:200, affinity), α-synuclein (α-syn) (1:200, affinity), and ACE2 (1:200, affinity) were detected using a DAB kit (catalog number: G1212, Servicebio). Immunofluorescence staining of nucleus with DAPI for 10 min. A microscope (Leica DMI4000B; Wetzlar, Germany) was used for the observation. Densitometry analysis was performed on scanned immunofluorescence and immunohistochemistry images using the ImageJ software.

Total Protein Extraction and Western Analysis

The SN and cells were lysed using RIPA buffer supplemented with PMSF (catalog numbers: G2002 and G2008; Servicebio). The lysate was sonicated and then cleared by centrifugation at 12,000×g for 10 minutes at 4°C. The protein concentration in the supernatant was determined using the BCA assay. The lysate was then separated on sodium dodecyl sulfate-polyacrylamide gel electrophoresis (SDS-PAGE) gels and transferred onto a nitrocellulose membrane (Millipore, IPFL00010, Germany) through electrophoresis. The membrane was blocked in 5% nonfat milk in TBST for 1 h at room temperature. Primary antibodies, including NF-κB (1:1000, Affinity), TH (1:500, Affinity), α-syn (1:1000, Affinity), ACE2 (1:1000, Affinity), and GAPDH (1:3000, Affinity), were incubated with the membrane in TBST with 1% nonfat milk overnight at 4°C. After overnight incubation, the membrane was incubated with HRP-conjugated secondary antibody in TBST with 1% nonfat milk for 2 h at room temperature. Following three cycles of 10 min TBST washes, the blots were detected using chemiluminescence (Bio-Rad). Densitometry analysis of scanned Western blot images was performed using ImageJ software. The timeline of MPTP induced PD mice model is shown in Figure 2.
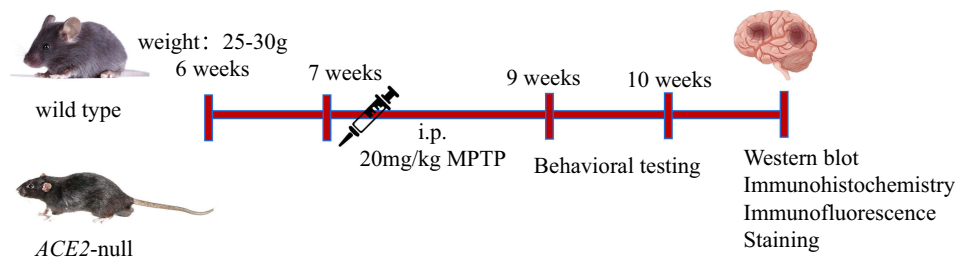
Figure 2 The timeline of MPTP induced PD mice model in vivo experiments.

Statistical Analysis

In this study, R adaptation 4.2.0 software and Adobe Photoshop 2021 were utilized. The data were expressed as the mean ± SEM, and group comparisons were conducted using an unpaired Student's *t*-test. The area under the ROC curve (AUC) and predictive accuracy were assessed. Statistical significance was defined as a *P*-value less 0.05.

Results

Differentially Expressed Gene Acquisition and Analysis

Normalization with samples from the GSE22491 and GSE164805 datasets using thresholds of adjusted *P-value* < 0.05. Volcano plots were used to visualize the differential genes, resulting in 1271 genes identified in the PD dataset GSE22491 and 3947 genes in the COVID-19 dataset GSE164805. PCA and mean-variance trend analysis indicated that the data were reproducible and lacked significant trends, as observed in the distribution patterns of boxplots (Figure 3A and B).

Immune Infiltration Analysis and GSEA

In the difference ranking plot (Figure 4A), the top five upregulated and downregulated genes were identified in the GSE22491 and the GSE164805 datasets. We further examined the correlation between the stromal and immune scores. In the GSE22491 dataset, there was a positive correlation between stromal and immune scores, whereas in the GSE164805 dataset, there was a negative correlation (Figure 4B). Heatmaps depicting immune cell infiltration in the GSE22491 and the GSE164805 datasets are shown in Figure 4C. Compared with the healthy controls, several immune cell types, including aDC, B cells, CD8 T cells,
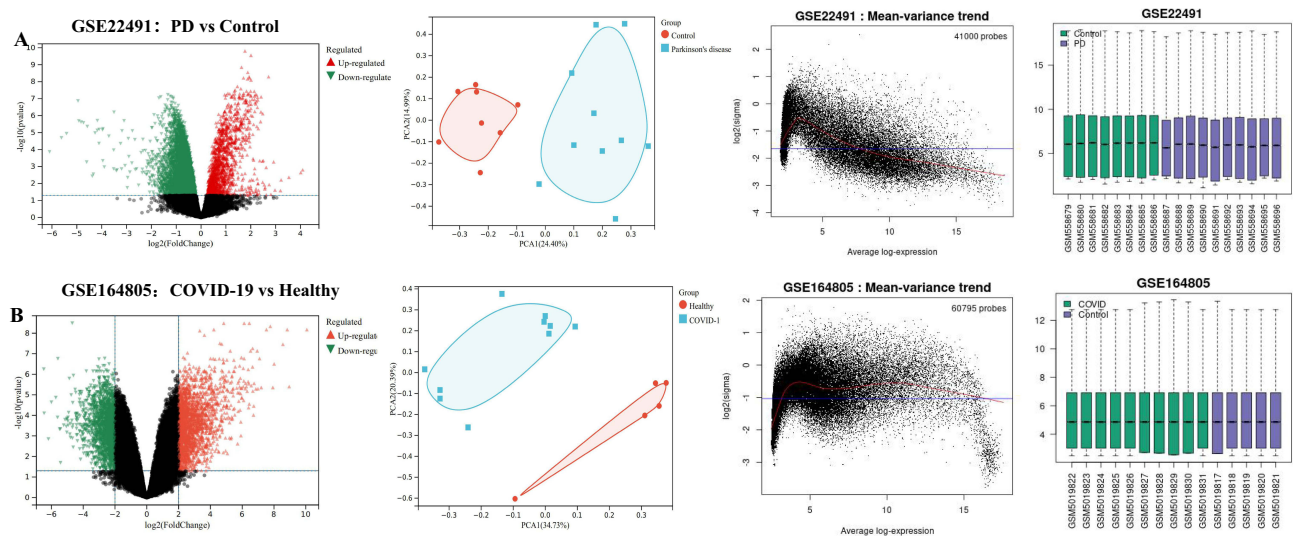

Figure 3 Gene chip data information. (**A**) Chip data of differential genes in PD compared with the healthy controls of the GSE22491. (**B**) Chip data of differential genes in COVID-19 compared with the healthy controls of GSE164805 datasets.
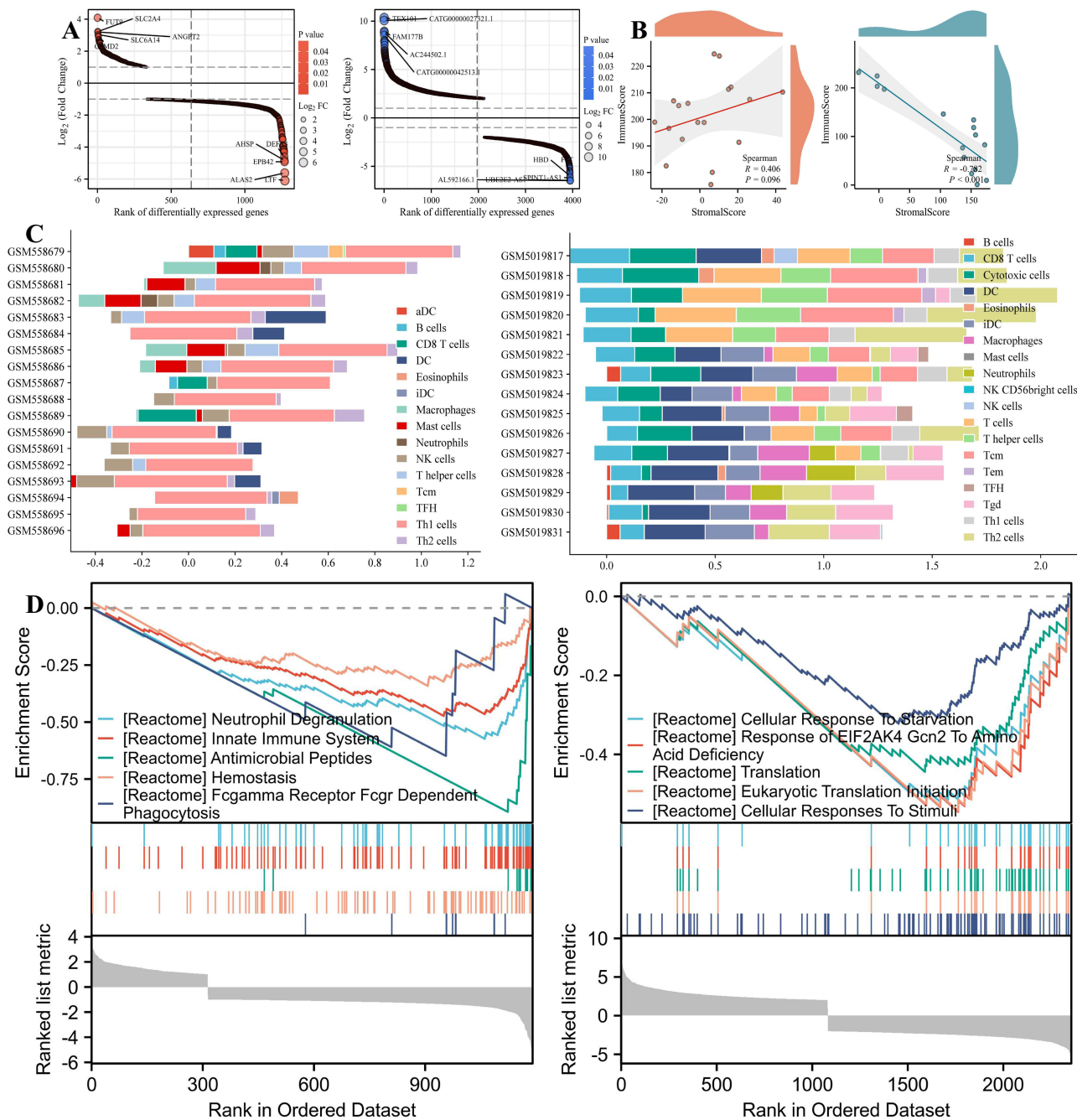
Figure 4 Differential expression gene analysis. (**A**) The difference ranking plot of DEG between the PD, COVID-19 and healthy controls in the GSE22491 and the GSE164805 datasets, up-regulated genes CSMD2, SLC6A14, ANGPT2, SLC2A4, FUT9, and down-regulated genes LTF, ALAS2, EPB42, AHSP, DEFA3 in the GSE22491 dataset; up-regulated genes CATG00000042513.1, AC244502.1, FAM177B, CATG00000027321.1, TEX101, and down-regulated genes AL592166.1, UBE2E2-AS1, SPINT1-AS1, HBD, FST in the GSE164805 dataset. (**B**) The correlation between the stromal scores and the immune scores in the GSE22491 and the GSE164805 datasets. (**C**) Boxplot of differentially expressed immune cells in the GSE22491 and the GSE164805 datasets. (**D**) GSEA enrichment analysis of the GSE22491 and the GSE164805 datasets.

Macrophages, Mast cells, Neutrophils, TFH, Th2 cells, Eosinophils, Tcm, and Th1 cells, were found to be expressed in PD in the GSE22491 dataset (Supplementary Figure S1A). Conversely, DC and NK cells were found to be highly expressed. In the GSE164805 dataset, compared with the healthy controls, CD8 T cells, cytotoxic cells, eosinophils, iDC, T cells, T helper cells, Tcm, Tgd, and Th2 cells were expressed at low levels in PD, while B cells, DC, mast cells, Neutrophils NK CD56bright cells were highly expressed (Supplementary Figure S1B). In the GSE22491 dataset, GSEA analysis revealed that differentially expressed gene (DEG) were primarily involved in neutrophil degranulation, the innate immune system, antimicrobial

peptides, hemostasis, and fcGR-dependent phagocytosis. In the GSE164805 dataset, the DEG were mainly associated with cellular response to starvation, response of EIF2AK4 gcn2 to amino acid deficiency, translation, eukaryotic translation initiation, and cellular responses to stimuli (Figure 4D).

WGCNA Identification of DEG

To ensure a more accurate scale-free network distribution, the power of the weight parameter in the adjacency matrix must be carefully selected. The power value was set between 1 and 30, and the corresponding correlation coefficient and average connectivity degree of the network were calculated for each value. A higher correlation coefficient (with a maximum of 1) indicates a closer resemblance to a scale-free network distribution; however, maintaining a certain level of gene connectivity is essential. Therefore, the power value should guarantee a sufficient degree of gene connectivity, while ensuring a large correlation coefficient. The power value used in the analysis was 18 (Figure 5A).
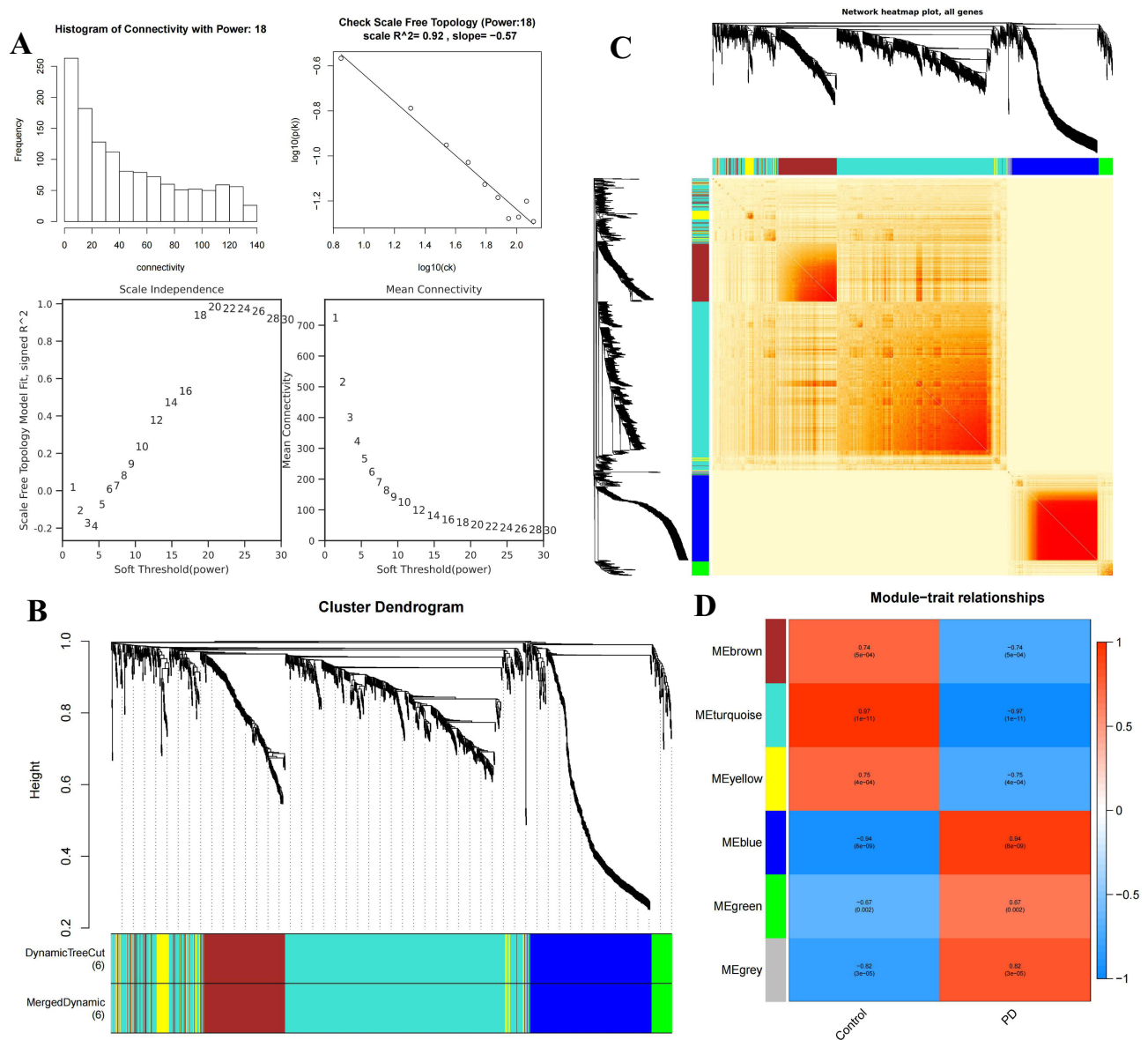

Figure 5 WGCNA analysis of the GSE22491 dataset. (**A**) WGCNA network construction parameters. (**B**) The upper middle part of the figure is the gene cluster tree constructed by the dissTOM matrix constructed by the weighted correlation coefficients. The color of Dynamic TreeCut is the module identified by the dynamicTreeCut method. Since there is a certain correlation between some modules, the corresponding modules are merged into the same module, that is, the merged dynamic below is the final module, and these modules are used for subsequent analysis. (**C**) Cluster heatmap of all genes. (**D**) Trait module association heatmap.

Using this selected power value, a weighted co-expression network model was established by dividing the 1271 genes into six modules. The Grey module represents genes that could not be assigned to any specific module and did not have any reference significance (Figure 5B). Figure 5C shows a clustering heatmap of all genes. Based on the results of the WGCNA module division, cluster plots, box plots, and bar charts were used to present module gene expression information (Supplementary Figure S2). By setting the threshold for the absolute value of the correlation coefficient to be greater than or equal to 0.3 and a *p*-value less 0.05, the modules related to each trait were identified (Figure 5D). Scatter plots were generated on the basis of these two values. The results indicated a high correlation between the genes in the module and both traits and characteristic genes within the module (Supplementary Figure S3). In total, 248 DEG were identified.

The power value used in the analysis was 30 (Figure 6A). The 3947 genes were divided into four modules. The gray module includes genes that could not be assigned to any module. No significant differences were observed between the groups (Figure 6B). Figure 6C shows a clustering heatmap for all genes. Supplementary Figure S4 shows module gene expression information using cluster plots, box plots, and bar charts based on the WGCNA module division results. Modules associated with each trait were identified (Figure 6D). Scatter plots were generated by calculating module gene expression and
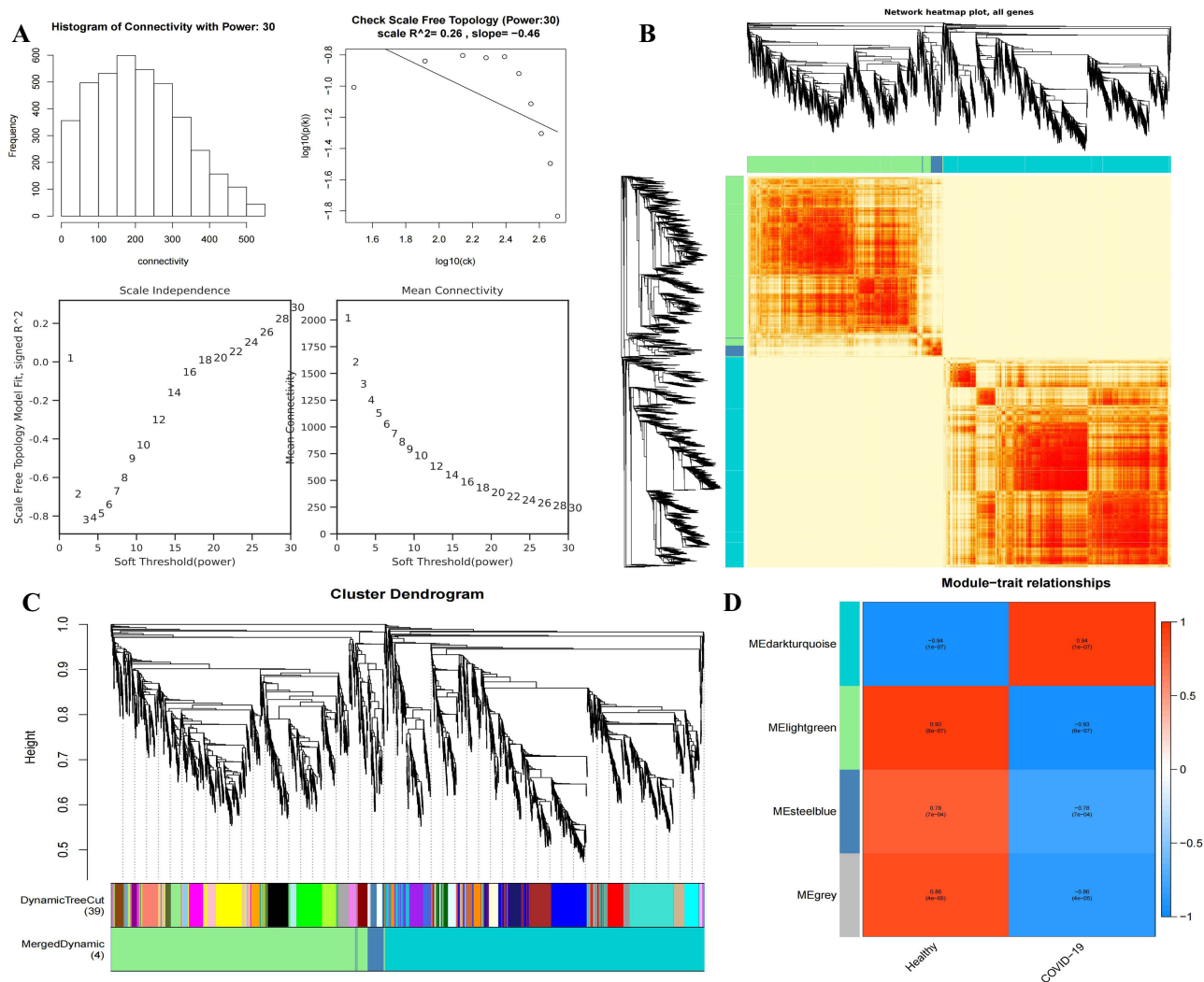

Figure 6 WGCNA analysis of GSE164805 dataset. (**A**) WGCNA network construction parameters. (**B**) The upper middle part of the figure is the gene cluster tree constructed by the dissTOM matrix constructed by the weighted correlation coefficients. The color of Dynamic TreeCut is the module identified by the dynamicTreeCut method. Since there is a certain correlation between some modules, the corresponding modules are merged into the same module, that is, the merged dynamic below is the final module, and these modules are used for subsequent analysis. (**C**) Cluster heatmap of all genes. (**D**) Trait module association heatmap.

eigengenes. The results indicated that the genes in the module were strongly correlated with both the traits and the feature genes in the module (Supplementary Figure S5). In total, 150 DEGs were identified in the COVID-19 dataset.

Differential Gene Analysis of Ibuprofen in Alleviating PD

In vitro evidence suggests that ibuprofen inhibits NF-κB may help reduce excessive inflammation or cytokine release in COVID-19 patients.[17] Due to the fact that inflammatory changes are also a cause of PD, the effects of anti-inflammatory drugs on PD have been widely studied to alleviate neuroinflammation. Previous studies have shown that the use of NSAIDs, especially ibuprofen, can reduce the risk of PD.[46] Therefore, we analyzed the differential genes involved in ibuprofen alleviating PD. Eleven targets were identified through the intersection of ibuprofen and PD, including down-regulated genes such as HDC, IGKV1-5, IGLJ3, PTGS1, SNCA, EGF, EIF4E, IGF1, and IGKC, and upregulated genes RELA and SIK1. Three targets were identified through the intersection ibuprofen and COVID-19, including the down-regulated genes, RELA, ZNF410, and RSL1D1 (Figures 7A–C). Figure 7D shows the expression levels and correlations between the 13 DEG in the GSE22491 dataset. GO and KEGG analysis were performed to reveal the potential biological functions and enriched pathways of the differentially expressed gene. Gene ontology analysis was divided into biological processes (BPs), cellular components (CCs), and molecular functions (MFs). The BP of the DEG were mainly enriched in the regulation of carbohydrate biosynthetic processes, regulation of carbohydrate metabolic processes, carbohydrate biosynthetic processes, positive regulation of carbohydrate metabolic processes, and receptor-mediated endocytosis (Figure 7E). The CC of DEG was mainly enriched in platelet alpha granules, platelet alpha granule lumen, platelet microparticles, immunoglobulin complexes, and mRNA cap-binding complexes (Figure 7F). The MF of the DEG was mainly enriched for transcription factor binding inhibitor, DNA binding transcription factor binding, growth factor activity, antigen binding, and protein kinase regulatory activity (Figure 7G). KEGG analysis showed that the DEG were mainly associated with the HIF-1 signaling pathway, EGFR tyrosine kinase inhibitor resistance, PI3K-AKT signaling pathway, MAPK signaling pathway, and Ras signaling pathway (Figure 7H). The biological functions of DEG are shown in Table 2.

Identification of Diagnostic Gene

Receiver operating characteristic (ROC) curves were used to evaluate the diagnostic value of the 13 hub genes for PD. Figures 8A and B show the diagnostic value of the 13 hub genes in the GSE22491 and the GSE164805 datasets, respectively. ROC analysis showed that the respective areas under the curve (AUCs) of PTGS1, IGLJ3, IGKV1-5, HDC, SIK1, IGKC, IGF1, EIF4E, EGF, SNCA, and RELA were 0.800, 0.875, 0.887, 0812, 1.000, 0.925, 0.912, 1.000, 0.725, 0.963, and 0.988 in the GSE22491 dataset. For the GSE164805 dataset, the RSL1D1, ZNF410, and RELA datasets were 1.000, 1.000, and 0.960, respectively. We used the validation dataset GSE49036 to verify the expression changes of DEG and the NFκB family in pathological stages (stage 0–6) again (Supplementary Figure S6), which was consistent with the results of the GSE22491 dataset. The expression of DEG and NF-κB family members was analyzed using the validation datasets GSE171110, GSE153970, and GSE175779 (Supplementary Figure S7).

Molecular Docking

To assess the binding affinity of the candidate drugs to their targets, we conducted molecular docking analysis. Autodock Vina v.1.2.2 was utilized to obtain the binding poses and interactions of ibuprofen with two proteins. The binding energy for each interaction was calculated (Figure 9 and Table 3). The findings revealed that the ibuprofen candidate forms visible hydrogen bonds and strong electrostatic interactions with its protein targets. Specifically, NF-κB and RELA exhibited binding energies of −7.451 kcal/mol and −4.999 kcal/mol, respectively, indicating a stable binding.

The Anti-Inflammatory Effect of Ibuprofen in PD Cell Model

To verify the anti-inflammatory effects of ibuprofen, the SH-SY5Y neurons induced by MPP$^+$ in vitro a PD model were treated with ibuprofen. Compared with the control group, MPP$^+$ treatment increased the expression of NF-κB p65, IL-1β, interleukin-6 (IL-6), and TNF-α ($P<0.05$). In contrast, compared with MPP$^+$, the expression of NF-κB p65, TNF-α, IL-1β, and IL-6 decreased after ibuprofen treatment ($P<0.05$). At the same time, we also detected the expression of PD
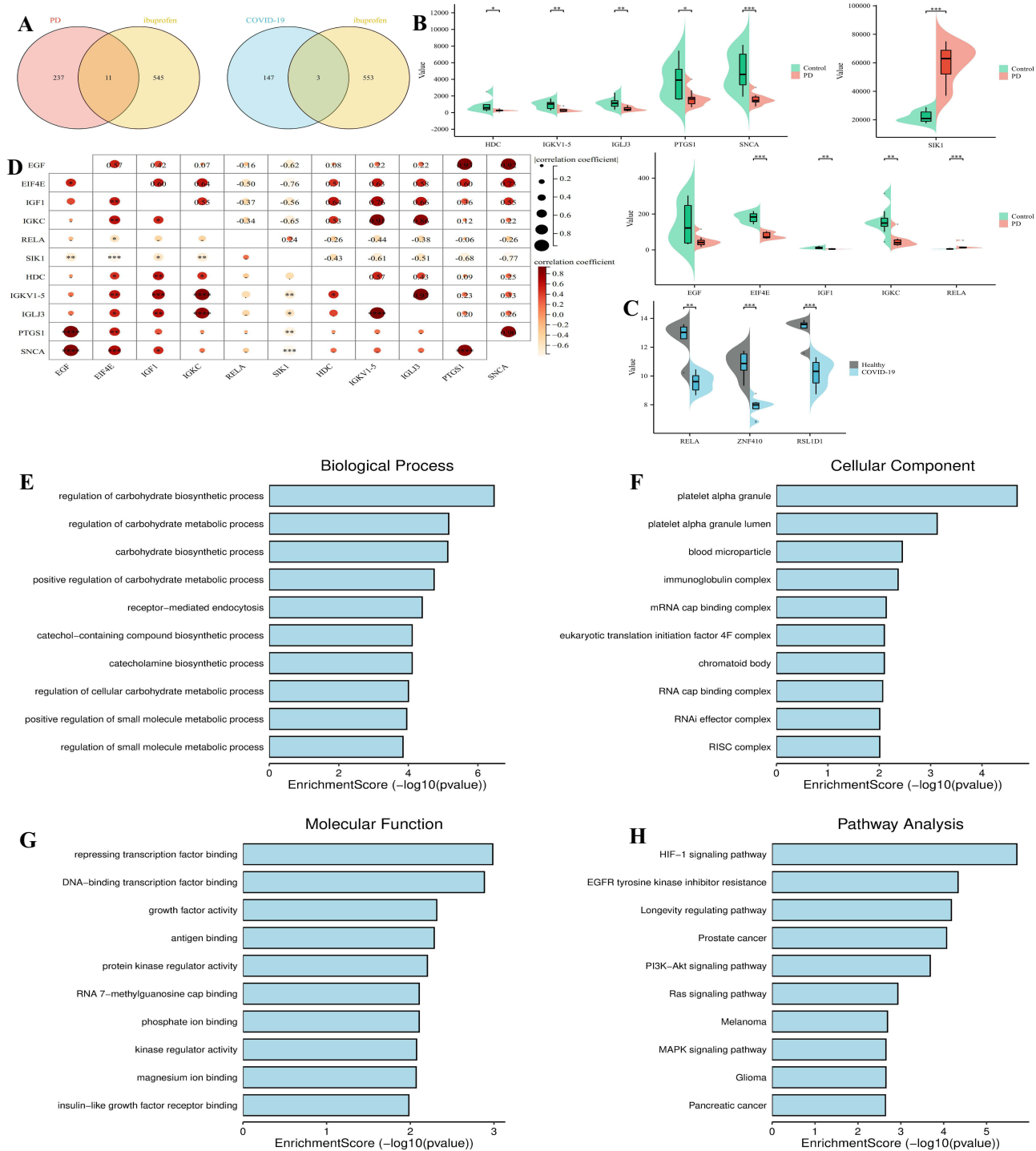
Figure 7 Overlapping gene analysis. (**A**) Venn diagram of overlapping genes between PD, COVID-19 and ibuprofen-related genes. (**B**) The box plot shows DEG expression in PD. (**C**) The box plot shows DEG expression in COVID-19. (**D**) Spearman correlation among 11 DEG in the GSE22491 dataset. Biological function and KEGG enrichment analysis, including (**E**) GOBP, (**F**) GOCC, (**G**) GOMF, and (**H**) Pathway. Compared with the healthy controls, *$P < 0.05$, **$P < 0.01$, ***$P < 0.001$.

indicators α-syn and TH, and compared with the control group, α-syn expression increased while TH expression decreased ($P<0.05$). Compared with the MPP⁺ group, α-syn expression decreased, TH expression increased after treatment with ibuprofen ($P<0.05$) (Figures 10A–G). The localization and fluorescence intensity of NF-κB p65 were detected using immunofluorescence. Compared with the control group, MPP⁺ significantly increased the average

Table 2 Biological Functional Analysis of Differentially Expressed Genes in PD and COVID-19

Protein	Biological function
PTGS1	Prostaglandin-Endoperoxide Synthase 1 (PTGS1) is an enzyme protein involved in regulating the production of prostaglandins in the body. Prostaglandin E2 is an important inflammatory mediator that plays a role in regulating immune responses during the inflammatory process. PTGS1 also participates in coordinating the release of hormones and neurotransmitters. Regulate the synthesis and release of precursor substances within dopamine cells. In addition, PTGS1 is also associated with oxidative stress and cell apoptosis.
EGF	Epidermal Growth Factor (EGF) can promote the growth and differentiation of nerve cells, helping to repair and restore the function of dopamine neurons. EGF also has antioxidant and anti-inflammatory effects. By inhibiting the release of inflammatory factors, reducing oxidative stress and inflammatory response, neurons are protected from damage. It can also promote the synthesis and release of neurotransmitters such as dopamine and acetylcholine, which may play a role in improving neurological function.
EIF4E	Eukaryotic Translation Initiation Factor 4E (EIF4E) is involved in regulating protein synthesis. PD is related to abnormal protein metabolism, including abnormal aggregation of α-syn and metabolic disorders of other proteins in neurons. EIF4E is associated with inflammatory response and oxidative stress. EIF4E may be associated with genetic risk factors for PD. Mutations in certain PD related genes can affect the expression or function of EIF4E, thereby participating in the regulation of the onset and development of PD.
SIK1	Salt-Inducible Kinase 1 (SIK1) plays an important regulatory role in neurons. It is involved in regulating the development, maturation, and function of neurons, and may also affect synaptic formation and plasticity in neurons. SIK1 also participates in regulating inflammatory response and cell apoptosis.
HDC	Histidine Decarboxylase (HDC) is responsible for catalyzing the conversion of histidine to histamine. In PD, HDC may play a role in neuroinflammation, oxidative stress, and movement disorders.
IGF1	Insulin-like Growth Factor 1 (IGF1) has neuroprotective and regenerative effects, promoting the survival and proliferation of nerve cells, and reducing neuronal death and damage. IGF1 can protect the survival and function of dopamine neurons through anti apoptotic, antioxidant, and anti-inflammatory pathways. IGF1 can also promote synaptic connections between neurons and the release of neurotransmitters.
IGKC	Immunoglobulin κ Constant (IGKC) may be related to the inflammatory response of the immune system, and immune inflammation plays an important role in neurological diseases. Some studies suggest that inflammatory responses may be involved in the pathophysiological processes of PD, including neuronal damage and inflammation mediated neurodegeneration. Therefore, IGKC may have an impact on the development and pathological process of PD by regulating the inflammatory response and immune regulation of the immune system.
IGKV1-5	Immunoglobulin Kappa Variable 1–5 (IGKV1-5) is involved in the immune response, and abnormal activation and inflammatory response of the immune system may be related to the occurrence and development of PD.
IGLJ3	Immunoglobulin Lambda Joining 3 (IGLJ3) is involved in the immune response.
SNCA	SNCA is a gene that encodes α-syn. The occurrence of SNCA gene mutations or abnormal aggregation of SNCA proteins can lead to the development of Parkinson's disease. These fibrous structures formed by abnormal aggregation are called Lewy bodies. SNCA is involved in regulating signal transmission between neurons, especially at the presynaptic terminals. SNCA has a high affinity for iron ions and can regulate intracellular iron metabolism. SNCA mutations may lead to abnormalities in the autophagy pathway, which in turn affects the clearance and accumulation of intracellular waste, ultimately leading to neuronal degeneration.
RELA	RELA is a gene encoding the NF-κB p65 subunit. NFB is an important transcription factor that participates in regulating biological processes such as cellular inflammation, immune response, and apoptosis. The activation and regulation of the NF-κB pathway are closely related to disease progression in PD and COVID-19.
ZNF410	Zinc Finger Protein 410 (ZNF410) is a transcription factor that can affect the expression of downstream genes, regulate cell cycle, differentiation, and development, and play a role in immune response.
RSL1D1	Ribosomal L1 Domain Containing 1 (RSL1D1) enables mRNA 3'-UTR binding activity and mRNA 5'-UTR binding activity. Involved in regulation of apoptotic process and regulation of cellular senescence. Regulates cellular senescence through inhibition of PTEN translation. Acts as a pro-apoptotic regulator in response to DNA damage.

fluorescence intensity of NF-κB p65 ($P<0.05$). However, compared with the MPP$^+$ group, the mean fluorescence intensity of NF-κB p65 decreased after ibuprofen treatment (Figures 10H and I).

Construction of the COVID-19 and PD Pathways Network

The Figure 11 demonstrates the COVID-19 and PD pathway network, which was constructed by integrating the aforementioned KEGG pathways. The RAS axis has been implicated in the progression of PD and other neurodegenerative diseases by promoting oxidative stress and neuroinflammation.[47,48] The population of dopaminergic neurons,
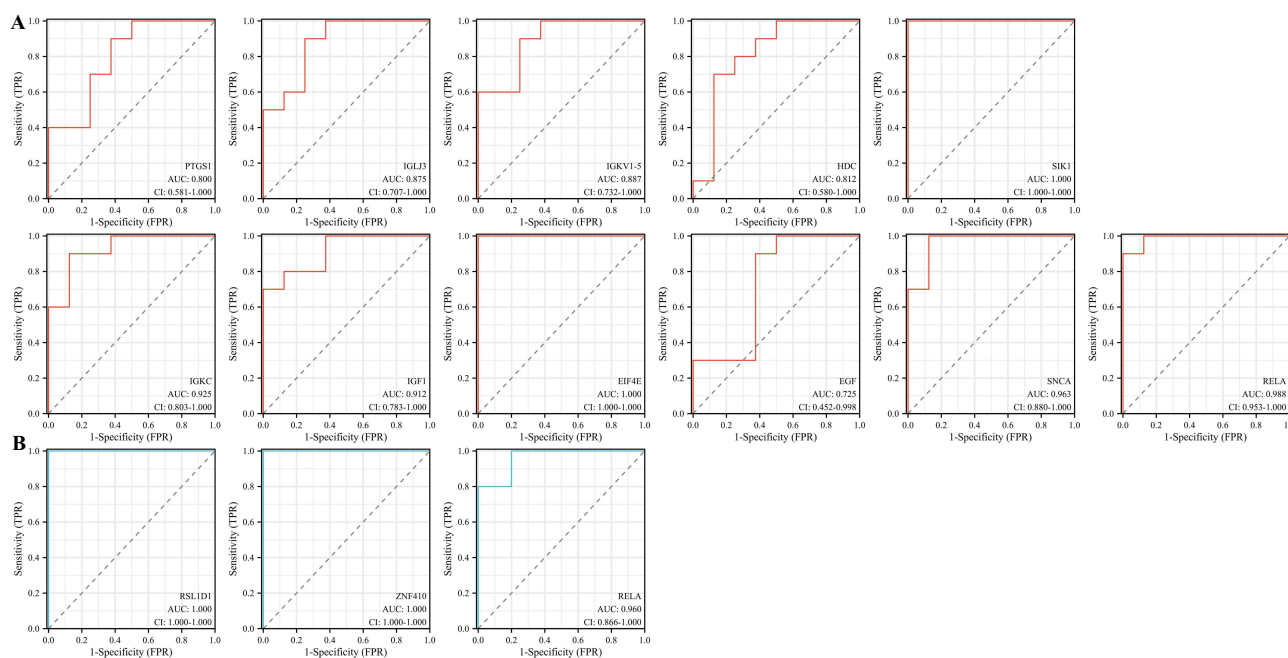
Figure 8 Diagnostic value of DEG in (**A**) the GSE22491 and (**B**) the GSE164805 datasets.

which is most susceptible to degeneration in PD, can be identified by the high expression of the AT1. The tissue RAS, including the brain RAS, comprises two opposing arms: a proinflammatory and prooxidative axis primarily mediated by Ang-II and AT1 receptors, and an anti-inflammatory and antioxidative axis composed of AngII/AT2 receptors along with Ang1-7/Mas receptors (MasR).[49,50] ACE2 converts peptides from the proinflammatory axis into peptides from the anti-inflammatory axis. The tissue RAS's significant role in inflammatory responses has recently been demonstrated in the context of the COVID-19 pandemic, as ACE2 is not only the entry receptor for SARS-CoV-2 but also a crucial component in the progression of COVID-19. Cytotoxicity induced by MPTP and other environmental toxins is mediated through the generation of reactive oxygen species (ROS), which attack neurons upon release. Additionally, these toxins stimulate complex intracellular signaling pathways in microglia involving mitogen-activated protein kinases (MAPKs) and NF-κB.[51] MAPKs, in turn, exert their actions on a wide array of genes involved in cellular responses to proinflammatory and other stress-related events. The regulatory effects of NF-κB on inflammation and immunity have dual aspects and may have opposite effects in different cellular contexts. The NF-κB pathway does regulate the production of proinflammatory cytokines, leukocyte recruitment, and cell survival, which are all critical factors in the inflammatory response.

Behavioral Test

Compared with the saline group, MPTP caused motor deficits, including a shorter footstep in the MPTP group ($P<0.01$) and a shorter footstep in the rotarod test (Supplementary Figure S8A). The MPTP group had a shorter fall time ($P<0.05$) (Supplementary Figure S8B). MPTP caused depression, including in the tail suspension test and forced swimming, and the immobility time of the MPTP group was prolonged ($P<0.05$) (Supplementary Figures S8C and S8D). MPTP caused anxiety in mice, including a reduction in the total distance moved ($P<0.05$) and a reduction in the time spent in the central area ($P<0.05$) in the open field test (Supplementary Figures S8E-S8G). In the elevated plus maze test, the MPTP group spent less time in the open-arm zone ($P<0.01$) (Supplementary Figures S8H and S8I). Compared with the MPTP group, *ACE2*-null mice in the a PD model increased in the above behavioral tests, indicating that *ACE2*-null mice increased the behavioral performance of PD.
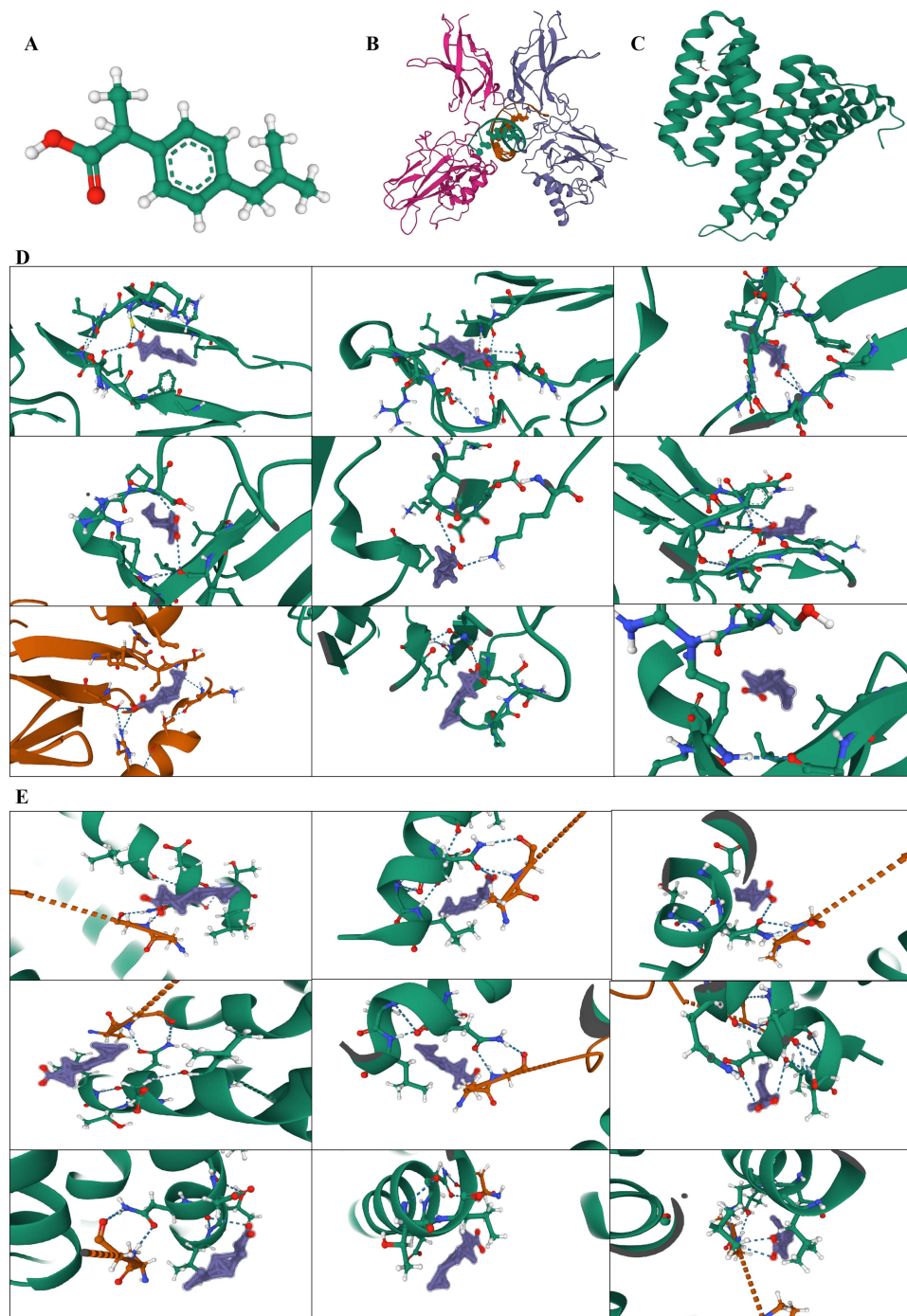
Figure 9 Binding mode of screened drugs to their targets by molecular docking. (**A**) Ibuprofen structure. (**B**) NFκB structure. (**C**) RELA structure. (**D**) Ibuprofen and NFκB binding mode. (**E**) Ibuprofen and RELA binding mode. Three-dimensional structures of the binding pockets were shown by PyMOL software.

Loss of Dopaminergic Neurons in MPTP-Induced PD Mice

TH plays an important role in PD, participating in the synthesis of dopamine. In PD, dopamine production in the SN is inhibited, leading to a decrease in dopamine levels. Therefore, we detected the expression of TH, and the after-effects of immunofluorescence and immunohistochemistry showed that compared with the saline group, the expression of TH was decreased in the MPTP group. Compared with the MPTP group, the decrease in TH was more significant in the MPTP induced *ACE2*-null mice (Figures 12A–D). The α-syn is a soluble protein expressed pre-synaptically and in the nucleus

Table 3 Binding Energy for Targets with Ibuprofen

Target	Drug	Binding energy (kcal/mol)	Acting force
1NFK	Ibuprofen	−7.451	HIS115, CYS116, ASN136
		−7.160	ASN136, GLY65
		−7.091	LEU67, ASN136
		−7.013	ILE139, SER63
		−6.977	LYS334, LYS275
		−6.839	ASN136, LEU67
		−6.795	ARG154, SER110
		−6.728	ILE139
		−6.626	–
6QHL		−4.999	–
		−4.951	ASN226
		−4.881	ASN226
		−4.790	–
		−4.789	–
		−4.597	ASP225
		−4.574	ASP225
		−4.549	–
		−4.416	GLY126

of the CNS. It is closely associated with the pathogenesis and related functional impairments of PD. Compared with the Saline group, the MPTP group showed apparent α-syn aggregation, and compared with the MPTP group, the aggregation of α-syn in the MPTP induced *ACE2*-null mice was significantly increased, and the average fluorescence intensity was enhanced (Figures 12E and F). MPTP- and MPTP-induced *ACE2*-null mice in the PD models showed a neuronal decline and decidedly added fluorescence acuteness (Figure 12G).

Role of ACE2 in PD

A decrease in ACE2 levels in patients with COVID-19 leads to inflammation and susceptibility to PD. The role of ACE2 in PD was analyzed using an MPTP-induced *ACE2*-null gene mouse model of PD. First, the tail DNA of *ACE2*-null mice was identified (Figure 13A). The distribution of ACE2 in the brain was analyzed, and the results showed that ACE2 was widely distributed in the brain. These include the SN, striatum, cerebellum, olfactory bulb, cortex, and hippocampus (Figures 13B–E). In the SN and striatum, compared with the Saline group, the expression of ACE2 and TH in MPTP-induced PD models decreased ($P<0.05$). Compared with the MPTP group, ACE2 was barely expressed in MPTP-induced *ACE2*-null mice. The expression of α-syn and NF-κB p65 was increased ($P<0.05$) (Figures 13F–J). And we found that there are differences in the content of ACE2 in different cells of the brain during fetal and adulthood, such as high expression of ACE2 in astrocytes cells in the adult brain and high expression of ACE2 in neuronal cells in the fetal brain (Supplementary Figure S9). These results indicate that PD pathology was more aggravated after *ACE2*-null, the expression of inflammatory factors increased more significantly, and *ACE2*-null was positively correlated with inflammation.

Discussion

It is important to closely monitor and provide medical guidance to COVID-19 patients, particularly those experiencing specific neurological symptoms such as persistent loss of smell (hyposmia), fainting (syncope), and persistent confusion. These symptoms are consistent with PD and PD dementia, although the prognosis for PD patients with COVID-19 is poor due to the complex nature of the disease's progression and the lack of specific treatments. In this study, we conducted an analysis using two datasets (PD and COVID-19) obtained from the GEO database and examined the DEGs. Through GO and KEGG pathway analyses, we identified GOBP categories associated with regulation of carbohydrate
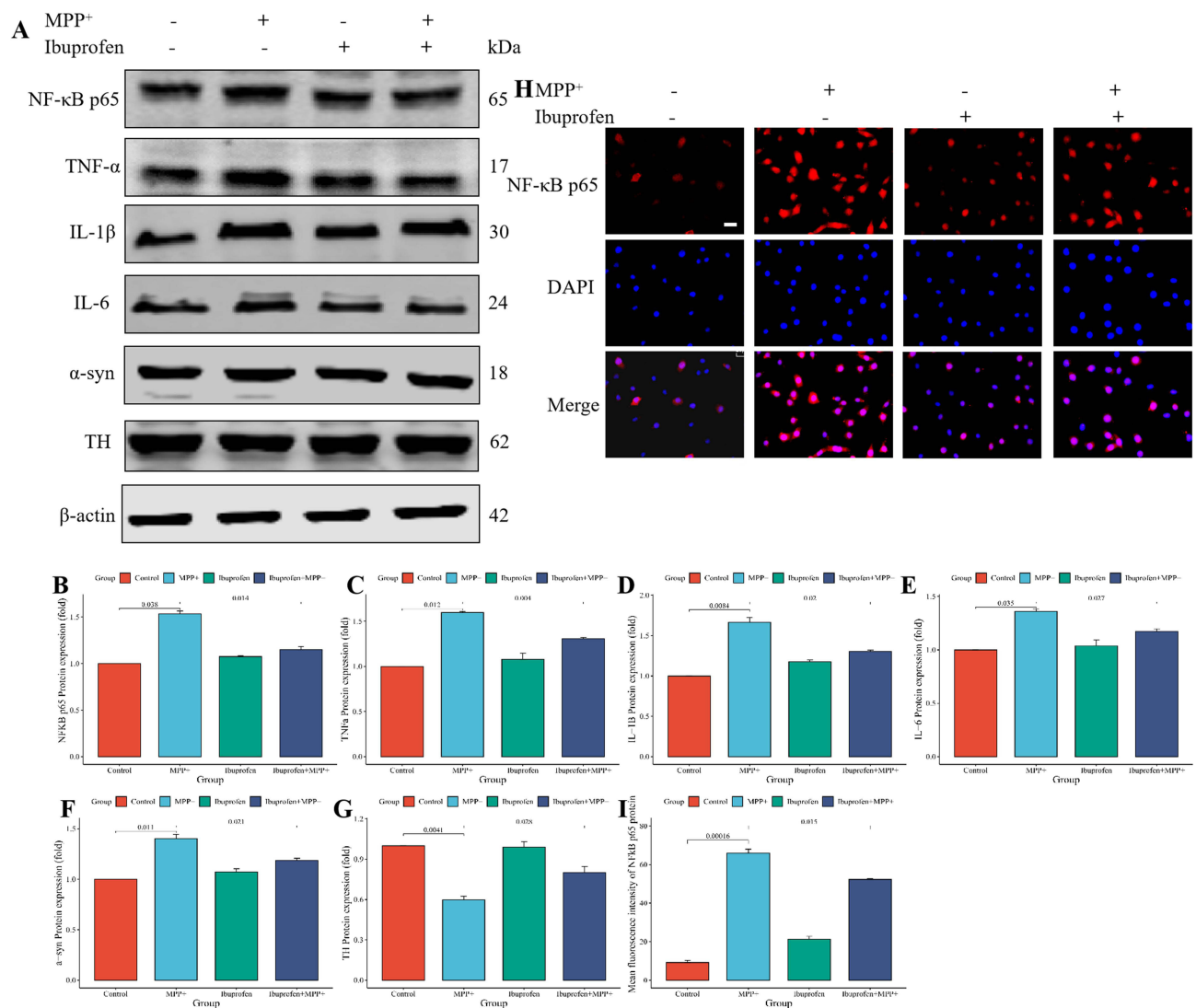
Figure 10 Ibuprofen inhibits MPP+ induced NF-κB signaling pathway expression in SH-SY5Y neurons. (**A**) NF-κB p65, TNF-α, IL-1β, and IL-6 protein expression in SH-SY5Y neurons. Statistical plots of (**B**) NF-κB p65, (**C**) TNF-α, (**D**) IL-1β, (**E**) IL-6, (**F**) α-syn, and (**G**) TH. (**H**) Immunofluorescence of NF-κB p65 protein. (**I**) Statistical plot of mean fluorescence intensity of NF-κB p65 protein (Scale bar, 20 μm), n=3.

biosynthesis and metabolism, as well as receptor-mediated endocytosis. KEGG pathway analysis revealed that the DEGs were mainly involved in the HIF-1 signaling pathway, EGFR tyrosine kinase inhibitor resistance, PI3K-AKT signaling pathway, MAPK signaling pathway, and Ras signaling pathway. We also found that immune cells are important in PD and COVID-19, such as cytotoxic cells, neutrophils, Th1, and Th2 cells. Studies has shown that, cytotoxic cells, such as cytotoxic T lymphocytes (CTLs) and natural killer (NK) cells,[52] play a crucial role in eliminating virus-infected cells in COVID-19.[53] In PD, cytotoxic cells may also contribute to neuroinflammation and neuronal damage.[54] The dysregulation of cytotoxic cells in PD combined with COVID-19 patients could exacerbate neurodegeneration and worsen the clinical outcomes. Neutrophils are the most abundant type of white blood cells and play a key role in the innate immune response. In COVID-19, excessive neutrophil activation can lead to cytokine storms and tissue damage. In PD, dysregulated neutrophil function may contribute to chronic inflammation and neurodegeneration.[55–57] The balance between Th1 and Th2 responses is crucial for immune homeostasis. In COVID-19, a shift towards a Th1 response is associated with pro-inflammatory cytokine release and tissue damage. In PD, dysregulation of Th1/Th2 balance has been implicated in neuroinflammation. In PD combined with COVID-19 patients, an imbalance towards Th1 response may exacerbate neuroinflammation and worsen disease progression.[58,59]
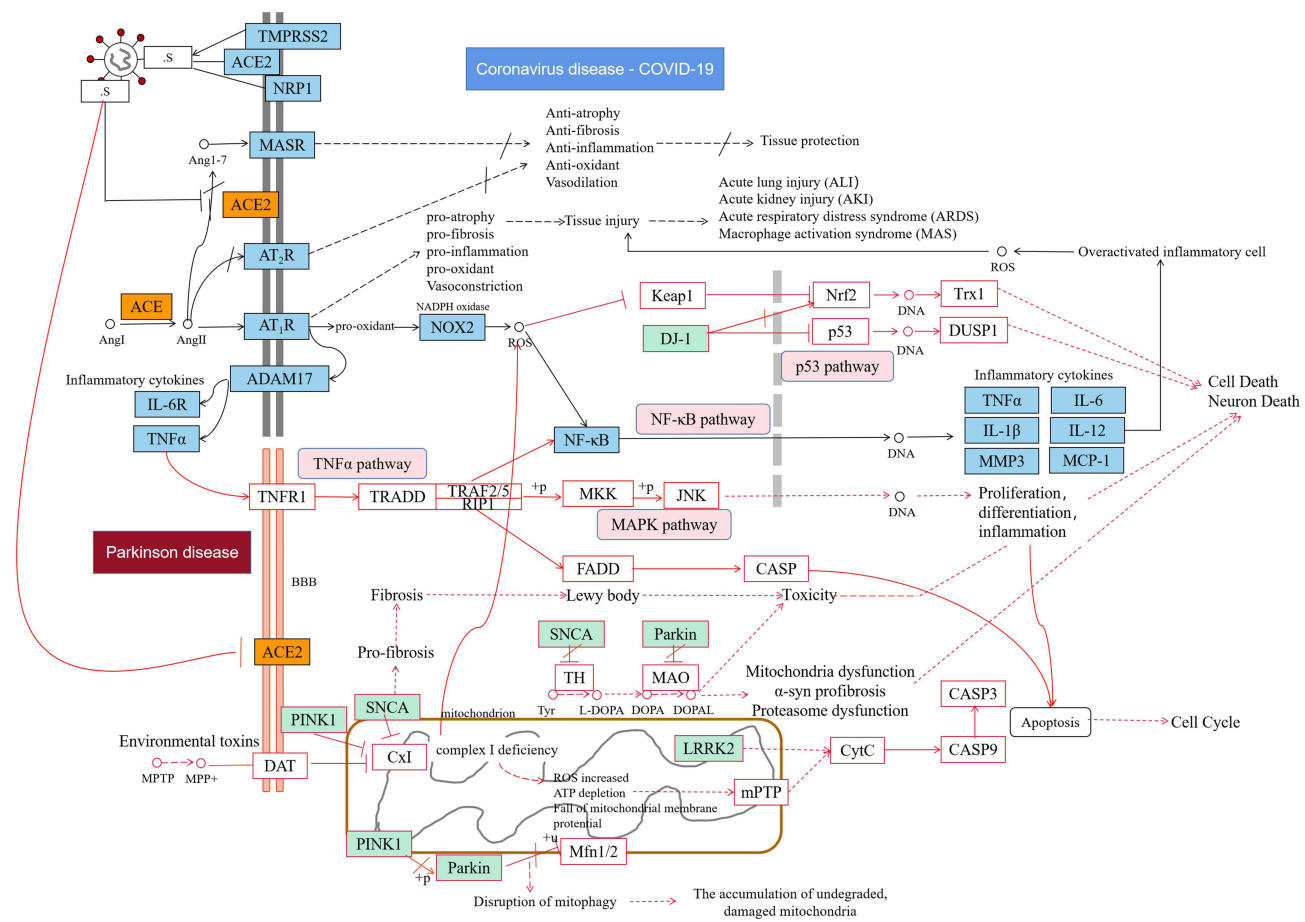
Figure 11 COVID-19 and PD pathways network. SNCA gene encoding α-syn is one of the key pathogenic genes of PD. The mutation of this gene can cause the overexpression of α-syn, and then form Lewy bodies, and inhibit the expression of tyrosine hydroxylase, thus blocking the synthesis of dopamine and leading to the occurrence of PD. The Parkin protein is responsible for degrading α-syn, and mutations cause the loss of Parkin function, which leads to the accumulation of α-syn. PINK1 protein interacts with α-syn at the end of the synapse, stabilizing the expression of α-syn, and PINK1 mutation leads to abnormal aggregation of α-syn. α-syn is considered to be one of the key mediators of PD caused by LRRK2 mutation. PARKIN and PINK1 are involved in the regulation of mitochondrial autophagy. In normal cells, PINK1 is selectively degraded by the proteasome, keeping its levels low. However, in damaged mitochondria, PINK1 accumulates on the mitochondrial outer membrane and recruits PARKIN to that site. The E3 ubiquitin ligase PARKIN then ubiquitinates proteins on the outer membrane of the mitochondria, marking the damaged mitochondria for degradation.

Our study has found that, ibuprofen can affect COVID-19 and PD by inhibiting NF-κB. RELA, as a crucial member of the NF-κB family, exerts precise control over the transcriptional activity of NF-κB through its post-translational modifications. This regulatory mechanism plays a pivotal role in various vital processes like inflammation, tumor progression, metabolism, immune response, and the pathogenesis of associated diseases. The post-translational modifications of RELA/p65 within the NF-κB pathway have been progressively unveiled, shedding light on their regulatory functions.[60,61] They play an important role in the occurrence and development of related diseases by regulating the protein-protein interactions, stability, and degradation of RELA, resulting in precise and complex regulation of the NF-κB pathway. Activation of the NF-κB p65 pathway after the activation of COX-2, IL-1β, and toll-like receptors in microglia leads to an added decline in dopaminergic neurons in the SN.[62] NFκB encodes the protein p105, which can be converted into p50 through proteasomal processing. The p50 protein frequently binds p65 to anatomy the archetypal approved NF-κB heterodimer, which is amenable to the activation of pro-inflammatory genes.[63] The clinical manifestations of COVID-19 primarily revolve around respiratory symptoms; however, emerging evidence suggests the presence of detrimental neurological symptoms as well. These include anosmia, dysgeusia, headaches, nausea, and vomiting.[64,65] Previous observations have indicated that approximately 36% of patients with COVID-19 exhibit neurological manifestations.[66] In the early stages of inflammation, protective immune responses are responsible for clearing viruses, so strategies to improve immune responses are important. As the disease progresses, pulmonary inflammation occurs due to the release of various pro-inflammatory cytokines such as IL-1β, IL-18, and IL-1 by
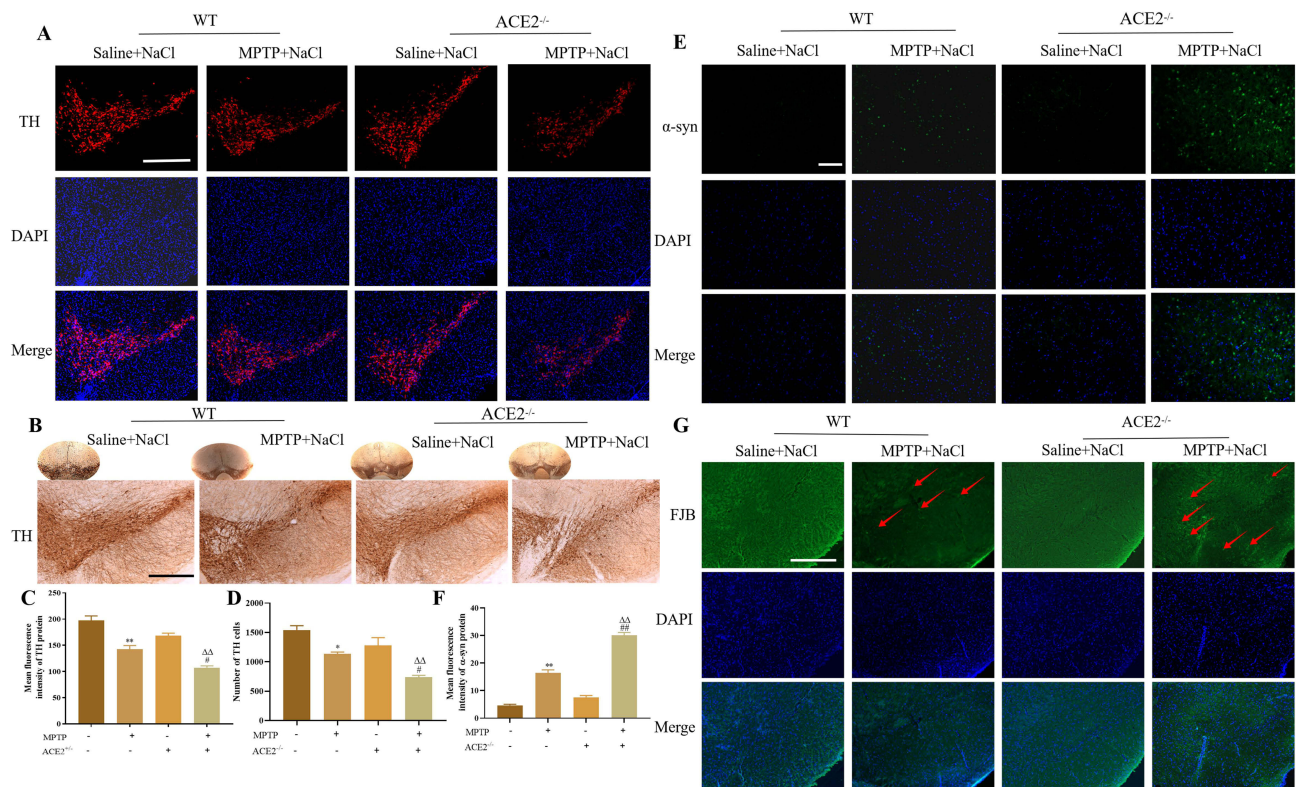
Figure 12 MPTP-induced neuronal loss in *ACE2*-null mice. (**A**) TH immunofluorescence (Scale bar, 100 μm). (**B**) TH immunohistochemistry (Scale bar, 100 μm). (**C**) Statistical plot of mean immunofluorescence intensity of TH. (**D**) Numbers of TH cells. (**E**) α-syn immunofluorescence (Scale bar, 50 μm). (**G**) FJB staining of degenerative neurons (Scale bar, 100 μm). Compared with the Saline group, $*P < 0.05$, $**P < 0.01$; Compared with the MPTP group, $\#P < 0.05$, $\#\#P < 0.01$; Compared with the *ACE2*-null group, $^{\triangle\triangle}P < 0.01$.

activated macrophages and Th1 cells.[67,68] However, elderly patients with comorbidities with different neurological problems have lower immune function and a higher risk of contracting COVID-19.[69] The virus can enter the CNS through various routes, including the blood, olfactory nerves (related to smell), and vagus nerves (which innervate organs in the chest and abdomen). In PD and COVID-19 patients, there seems to be a close relationship between inflammation and oxidative stress. The primary inflammatory signals trigger the release of microbial particles and cytokines. This activation leads to the activation of intracellular signaling pathways involving proteins like MAPK, NF-κB, janus kinase-signal transducer and activator of transcription (JAK-STAT).[70] At the same time, we also found that ibuprofen plays a role in PD and COVID-19 by affecting these genes, including HDC, IGKV1-5, IGLJ3, PTGS1, SNCA, EGF, EIF4E, IGF1, IGKC, SIK1, ZNF410, RSL1D1, and RELA These genes are involved in functions such as inflammation, oxidative stress, cell apoptosis, and immunity, and are crucial in the development of PD and COVID-19.

Many potential mechanisms have been suggested to explain the impact of COVID-19 infection on the development and progression of PD. A recent comprehensive review has excellently summarized these mechanisms.[71] Firstly, severe infection with SARS-CoV-2 has the potential to cause parkinsonism by damaging the nigrostriatal system through vascular injury. Secondly, the relationship between inflammation and the risk of PD suggests that severe neuroinflammation could lead to the degeneration of DAergic neurons in the SN, which are particularly susceptible to systemic inflammation. Finally, the presence of viral RNA in the brains of certain deceased COVID-19 patients supports the possibility of SARS-CoV-2 having neurotropic properties.[72] Pathological studies have found that secondary damage to PD extensively affects CNS structures such as the telencephalon (striatum, cerebral cortex, hippocampal), diencephalon (dorsal thalamus), brainstem (red nucleus, raphe nucleus), cerebellum (dentate nucleus), and spinal cord (anterior horn cells). The striatum, cerebral cortex, dorsal thalamus, and SN neural circuits are important information feedback circuits closely related to movement. Secondary consequential damages to the striatum, cerebral cortex, and dorsal thalamus will exacerbate the symptoms and signs of PD motor disorders. The cerebral cortex and hippocampus are currently recognized as important CNS structures for cognition, learning, and
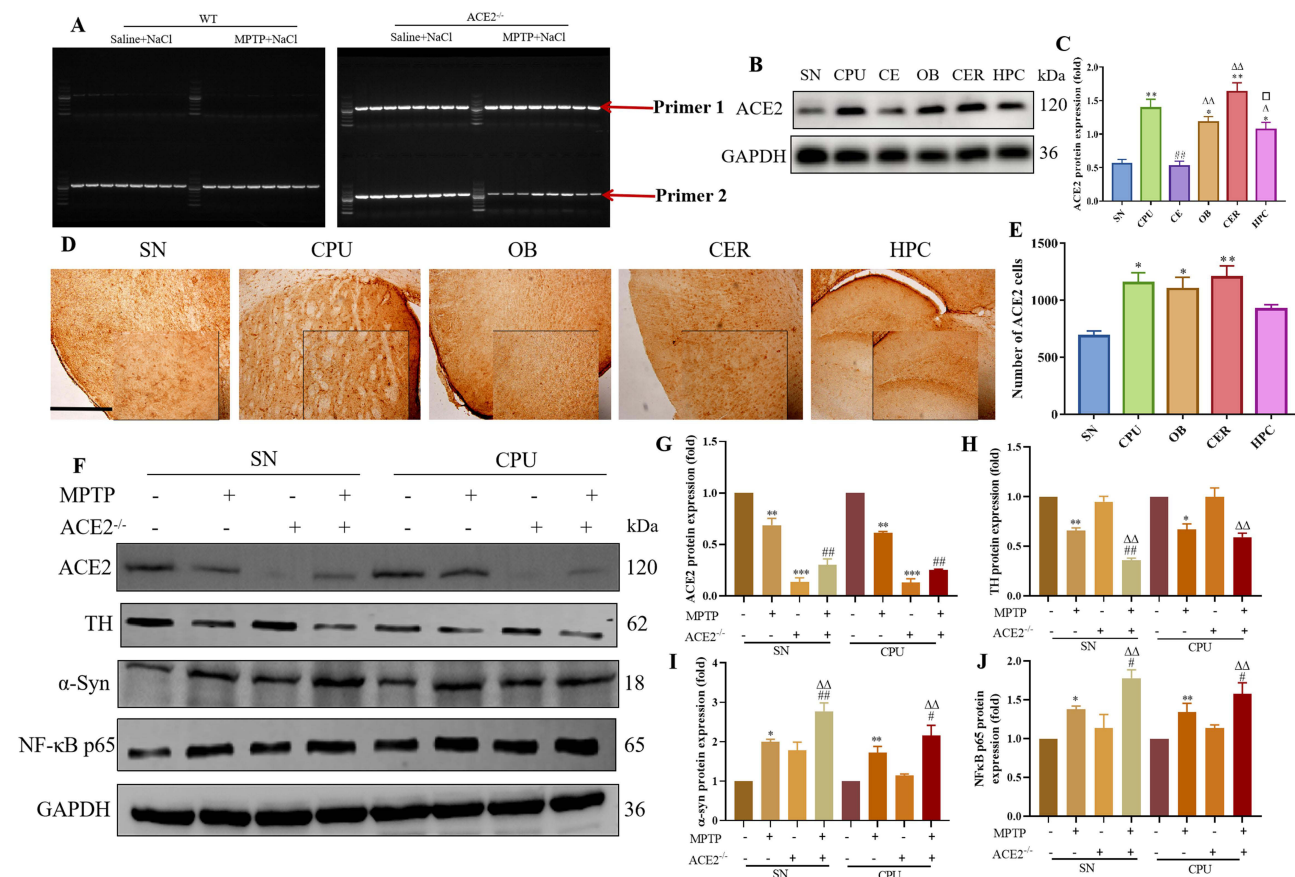
Figure 13 Protein expression in MPTP-induced *ACE2*-null mice. (**A**) Tail identification of *ACE2*-null mice. (**B**) ACE2 distribution in SN, striatum (CPU), cerebellum (CE), olfactory bulb (OB), cerebral cortex (CER), and hippocampus (HPC). (**C**) Statistical plot of ACE2 distribution in brain regions. (**D**) Immunohistochemical staining of ACE2 distribution in brain regions (Scale bar, 100 μm). (**E**) immunohistochemical cell numbers of ACE2 in brain regions. (**F**) Expression of ACE2, TH, α-syn, and NF-κB p65 proteins in striatum and SN in MPTP-induced *ACE2*-null mice. (**G**)-(**J**) Statistical plot of ACE2, TH, α-syn, and NF-κB p65 protein expression. Compared with the SN, *$P <$ 0.05, **$P < 0.01$; Compared with the CPU, #$P < 0.05$, ##$P < 0.01$; Compared with the CE, $^{\Delta}P < 0.05$, $^{\Delta\Delta}P < 0.01$; Compared with the CER, $^{\square}P < 0.01$. Compared with the Saline group, *$P < 0.05$, **$P < 0.01$, ***$P < 0.001$; Compared with the MPTP group, #$P < 0.05$, ##$P < 0.01$; Compared with the *ACE2*-null group, $^{\Delta\Delta}P < 0.01$.

memory. Secondary consequential damages to them can cause symptoms and signs such as perceptual, recognition, and memory impairments, and in severe cases, dementia.[73,74]

In the brain, SARS-CoV-2 may interact with ACE2 and other promoting receptors and spread through cellular adsorption and absorption.[75] ACE2, as a critical element of the RAS, plays a pivotal role in cardiovascular regulation and also exerts a significant influence on inflammatory responses in various tissues, including the brain.[76] In the brain, excessive activation of the RAS system has been associated with oxidative stress, inflammation, immune dysfunction, and abnormal cell growth and proliferation.[77] Furthermore, the presence of ACE2 mRNA and protein has been confirmed in the brainstem of mice, indicating that ACE2 is a novel component of the brain's RAS. Importantly, these findings signify that the involvement of ACE2 in the central nervous system extends beyond its role in cardiovascular function.[78] The binding of the COVID-19 virus to ACE2 can lead to downregulation of ACE2 and disruption of the ACE2/Ang(1–7)/MasR pathway, which might contribute to the pathogenesis of COVID-19.[79] Interestingly, ACE2 has also been implicated in the pathogenesis of PD. The dysfunction of ACE2 in PD has been linked to oxidative stress, neuroinflammation, disrupted mitochondrial function, abnormal protein accumulation, dysregulated autophagy, impaired apoptotic mechanisms, and imbalanced gut microbiota. These factors are believed to play a role in the initiation and progression of PD.[80] This study showed that *ACE2*-null mice exhibited more pronounced anxiety, depression, and movement disorders, as well as aggravated inflammation, leading to neuronal loss and significant aggregation of α-syn. Therefore, the search for drugs targeting ACE2 and understanding the mechanisms involved in PD could potentially lead to new therapeutic approaches for treating the disease. Exploring the possible connections between COVID-19 symptoms (such as hyposmia or anosmia, gastrointestinal symptoms, autonomic dysfunction) and the onset of PD, as well as investigating the role of ACE2 levels or autoantibodies in this context, could provide valuable insights.

In summary, our analysis indicates that the NF-κB signaling pathway plays a role in PD and COVID-19. The activation of this pathway seems to be a common response in the development of these two diseases. However, inhibiting this pathway may interfere with normal cellular function. We need further research to identify specific proteins and develop safe biological therapies to block the activation of NF-κB, thereby affecting other cellular processes. In general, continuous research on the relationship between COVID-19, ACE2 mediated inflammation and PD can reveal new treatment strategies to manage PD and related diseases. However, in the current study, we did not validate the COVID-19 combined with PD model, which is one of the limitations of our research. Despite the available information on the correlation between COVID-19 and neurological disorders, additional investigation is warranted to precisely determine the association between COVID-19 and PD. Hence, it is imperative to deepen our understanding of the underlying molecular mechanisms by establishing in vitro and in vivo models that incorporate the interaction between COVID-19 and PD. Furthermore, it is crucial to analyze clinical cohorts, conduct longitudinal studies, and carry out interventional clinical trials involving PD patients who have contracted COVID-19, in order to gain a more comprehensive insight into their relationship.

Conclusion

A connection between COVID-19 and PD has been established based on shared mechanisms. The neuroanatomy associated with PD exhibits a pro-inflammatory environment, oxidative stress, dysregulated autophagy, mitochondrial dysfunction, and ACE2 downregulation, which may amplify the adverse effects of SARS-CoV-2. Conversely, SARS-CoV-2 infection has the potential to initiate PD-related pathways through neuroinflammation, autophagy dysregulation, oxidative stress, disruption of the BBB, and ACE2 downregulation. This mutual interaction paves the way for further investigations into the underlying molecular mechanisms linking the two diseases and the development of targeted therapies.

Data Sharing Statement

All data and materials generated or analyzed during this study are included in this published article [and its supplementary information files].

Ethics Approval

This study was approved by the Ethics Committee of Henan University (no. HUSOM2015-37).

Author Contributions

All authors made a significant contribution to the work reported, whether that is in the conception, study design, execution, acquisition of data, analysis and interpretation, or in all these areas; took part in drafting, revising or critically reviewing the article; gave final approval of the version to be published; have agreed on the journal to which the article has been submitted; and agree to be accountable for all aspects of the work.

Funding

Disclosure

The authors declare no conflicts of interest regarding the publication of this paper.

References

1. Chuang HJ, Lin CW, Hsiao MY, Wang TG, Liang HW. Long COVID and rehabilitation. *J Formos Med Assoc*. 2024;123:S61–S69. doi:10.1016/j.jfma.2023.03.022
2. Andalib S, Biller J, Di Napoli M, et al. Peripheral nervous system manifestations associated with COVID-19. *Curr Neurol Neurosci Rep*. 2021;21(3):9. doi:10.1007/s11910-021-01102-5
3. Asadi-Pooya AA, Simani L. Central nervous system manifestations of COVID-19: a systematic review. *J Neurol Sci*. 2020;413:116832. doi:10.1016/j.jns.2020.116832

4. Rosen B, Kurtishi A, Vazquez-Jimenez GR, Møller SG. The intersection of parkinson's disease, viral infections, and COVID-19. *Mol Neurobiol*. 2021;58(9):4477–4486. doi:10.1007/s12035-021-02408-8

5. Zhou P, Yang XL, Wang XG, et al. A pneumonia outbreak associated with a new coronavirus of probable bat origin. *Nature*. 2020;579 (7798):270–273. doi:10.1038/s41586-020-2012-7

6. Hoffmann M, Kleine-Weber H, Schroeder S, et al. SARS-CoV-2 Cell Entry Depends on ACE2 and TMPRSS2 and Is blocked by a clinically proven protease inhibitor. *Cell*. 2020;181(2):271–280.e8. doi:10.1016/j.cell.2020.02.052

7. Aghagoli G, Gallo Marin B, Katchur NJ, Chaves-Sell F, Asaad WF, Murphy SA. Neurological Involvement in COVID-19 and Potential Mechanisms: a Review. *Neurocrit Care*. 2021;34(3):1062–1071. doi:10.1007/s12028-020-01049-4

8. Rai SN, Tiwari N, Singh P, et al. Exploring the Paradox of COVID-19 in Neurological Complications with Emphasis on Parkinson's and Alzheimer's Disease. *Oxid Med Cell Longev*. 2022;2022:3012778. doi:10.1155/2022/3012778

9. Merello M, Bhatia KP, Obeso JA. SARS-CoV-2 and the risk of Parkinson's disease: facts and fantasy. *Lancet Neurol*. 2021;20(2):94–95. doi:10.1016/S1474-4422(20)30442-7

10. Singh N, Rai SN, Singh V, Singh MP. Molecular characterization, pathogen-host interaction pathway and in silico approaches for vaccine design against COVID-19. *J Chem Neuroanat*. 2020;110:101874. doi:10.1016/j.jchemneu.2020.101874

11. Rinott E, Kozer E, Shapira Y, Bar-Haim A, Youngster I. Ibuprofen use and clinical outcomes in COVID-19 patients. *Clin Microbiol Infect*. 2020;26 (9):1259.e5–1259.e7. doi:10.1016/j.cmi.2020.06.003

12. Laughey W, Lodhi I, Pennick G, et al. Ibuprofen, other NSAIDs and COVID-19: a narrative review. *Inflammopharmacology*. 2023;31 (5):2147–2159. doi:10.1007/s10787-023-01309-7

13. Esposito E, Di Matteo V, Benigno A, Pierucci M, Crescimanno G, Di Giovanni G. Non-steroidal anti-inflammatory drugs in Parkinson's disease. *Exp Neurol*. 2007;205(2):295–312. doi:10.1016/j.expneurol.2007.02.008

14. Singh A, Tripathi P, Singh S. Neuroinflammatory responses in Parkinson's disease: relevance of Ibuprofen in therapeutics. *Inflammopharmacology*. 2021;29(1):5–14. doi:10.1007/s10787-020-00764-w

15. Krappmann D, Scheidereit C. A pervasive role of ubiquitin conjugation in activation and termination of IkappaB kinase pathways. *EMBO Rep*. 2005;6(4):321–326. doi:10.1038/sj.embor.7400380

16. Hirano T, Murakami M. COVID-19: A new virus, but a familiar receptor and cytokine release syndrome. *Immunity*. 2020;52(5):731–733. doi:10.1016/j.immuni.2020.04.003

17. Smart L, Fawkes N, Goggin P, et al. A narrative review of the potential pharmacological influence and safety of ibuprofen on coronavirus disease 19 (COVID-19), ACE2, and the immune system: a dichotomy of expectation and reality. *Inflammopharmacology*. 2020;28(5):1141–1152. doi:10.1007/s10787-020-00745-z

18. Khoshnood RJ, Zali A, Tafreshinejad A, et al. Parkinson's disease and COVID-19: a systematic review and meta-analysis. *Neurol Sci*. 2022;43 (2):775–783. doi:10.1007/s10072-021-05756-4

19. Sulzer D, Antonini A, Leta V, et al. COVID-19 and possible links with Parkinson's disease and parkinsonism: from bench to bedside. *NPJ Parkinsons Dis*. 2020;6:18. doi:10.1038/s41531-020-00123-0

20. Fearon C, Fasano A. Parkinson's Disease and the COVID-19 Pandemic. *J Parkinsons Dis*. 2021;11(2):431–444. doi:10.3233/JPD-202320

21. Gagne JJ, Power MC. Anti-inflammatory drugs and risk of Parkinson disease: a meta-analysis. *Neurology*. 2010;74(12):995–1002. doi:10.1212/WNL.0b013e3181d5a4a3

22. Chaudhry ZL, Klenja D, Janjua N, Cami-Kobeci G, Ahmed BY. COVID-19 and Parkinson's Disease: shared inflammatory pathways under oxidative Stress. *Brain Sci*. 2020;10(11):807. doi:10.3390/brainsci10110807

23. Mohammed M, Berdasco C, Lazartigues E. Brain angiotensin converting enzyme-2 in central cardiovascular regulation. *Clin Sci*. 2020;134 (19):2535–2547. doi:10.1042/CS20200483

24. Nakagawa P, Gomez J, Grobe JL, Sigmund CD. The Renin-Angiotensin System in the Central Nervous System and Its Role in Blood Pressure Regulation. *Curr Hypertens Rep*. 2020;22(1):7. doi:10.1007/s11906-019-1011-2

25. Hernández VS, Zetter MA, Guerra EC, et al. ACE2 expression in rat brain: implications for COVID-19 associated neurological manifestations. *Exp Neurol*. 2021;345:113837. doi:10.1016/j.expneurol.2021.113837

26. Beitz JM. Parkinson's disease: a review. *Front Biosci*. 2014;6(1):65–74. doi:10.2741/s415

27. Angelopoulou E, Bougea A, Papageorgiou SG, Villa C. Psychosis in Parkinson's Disease: A Lesson from Genetics. *Genes*. 2022;13(6):1099. doi:10.3390/genes13061099

28. Cilia R, Bonvegna S, Straccia G, et al. Effects of COVID-19 on Parkinson's Disease Clinical Features: a Community-Based Case-Control Study. *Mov Disord*. 2020;35(8):1287–1292. doi:10.1002/mds.28170

29. Antonini A, Leta V, Teo J, Chaudhuri KR. Outcome of Parkinson's Disease Patients Affected by COVID-19. *Mov Disord*. 2020;35(6):905–908. doi:10.1002/mds.28104

30. Anghelescu A, Onose G, Popescu C, et al. Parkinson's Disease and SARS-CoV-2 Infection: particularities of Molecular and Cellular Mechanisms Regarding Pathogenesis and Treatment. *Biomedicines*. 2022;10(5):1000. doi:10.3390/biomedicines10051000

31. Lukiw WJ. SARS-CoV-2, the Angiotensin Converting Enzyme 2 (ACE2) Receptor and Alzheimer's disease. *J Alzheimers Dis Parkinsonism*. 2021;11(4):520.

32. Barrett T, Wilhite SE, Ledoux P, et al. NCBI GEO: archive for functional genomics data sets--update. *Nucleic Acids Res*. 2013;41(Database issue): D991–5. doi:10.1093/nar/gks1193

33. Yoshihara K, Shahmoradgoli M, Martínez E, et al. Inferring tumour purity and stromal and immune cell admixture from expression data. *Nat Commun*. 2013;4:2612. doi:10.1038/ncomms3612

34. Hänzelmann S, Castelo R, Guinney J. GSVA: gene set variation analysis for microarray and RNA-seq data. *BMC Bioinf*. 2013;14:7. doi:10.1186/1471-2105-14-7

35. Bindea G, Mlecnik B, Tosolini M, et al. Spatiotemporal dynamics of intratumoral immune cells reveal the immune landscape in human cancer. *Immunity*. 2013;39(4):782–795. doi:10.1016/j.immuni.2013.10.003

36. Yu G, Wang LG, Han Y, He QY. clusterProfiler: an R package for comparing biological themes among gene clusters. *OMICS*. 2012;16(5):284–287. doi:10.1089/omi.2011.0118

37. Morris GM, Huey R, Olson AJ. Using AutoDock for ligand-receptor docking. *Curr Protoc Bioinformatics*. 2008. doi:10.1002/0471250953. bi0814s24

38. Wang Y, Bryant SH, Cheng T, et al. PubChem BioAssay: 2017 update. *Nucleic Acids Res*. 2017;45(D1):D955–D963. doi:10.1093/nar/gkw1118

39. Zhao M, Chen J, Mao K, et al. Mitochondrial calcium dysfunction contributes to autophagic cell death induced by MPP+ via AMPK pathway. *Biochem Biophys Res Commun*. 2019;509(2):390–394. doi:10.1016/j.bbrc.2018.12.148

40. Rymut SM, Kampman CM, Corey DA, Endres T, Cotton CU, Kelley TJ. Ibuprofen regulation of microtubule dynamics in cystic fibrosis epithelial cells. *Am J Physiol Lung Cell Mol Physiol*. 2016;311(2):L317–27. doi:10.1152/ajplung.00126.2016

41. Rai SN, Singh P. Advancement in the modelling and therapeutics of Parkinson's disease. *J Chem Neuroanat*. 2020;104:101752. doi:10.1016/j. jchemneu.2020.101752

42. Lu KT, Ko MC, Chen BY, et al. Neuroprotective effects of resveratrol on MPTP-induced neuron loss mediated by free radical scavenging. *J Agric Food Chem*. 2008;56(16):6910–6913. doi:10.1021/jf8007212

43. Zhu X, Dong J, Han B, et al. Neuronal Nitric Oxide Synthase Contributes to PTZ Kindling-Induced Cognitive Impairment and Depressive-Like Behavior. *Front Behav Neurosci*. 2017;11:203. doi:10.3389/fnbeh.2017.00203

44. Rial D, Castro AA, Machado N, et al. Behavioral phenotyping of Parkin-deficient mice: looking for early preclinical features of Parkinson's disease. *PLoS One*. 2014;9(12):e114216. doi:10.1371/journal.pone.0114216

45. Malloul H, Mahdani FM, Bennis M, S B-M. Prenatal exposure to paint thinner alters postnatal development and behavior in mice. *Front Behav Neurosci*. 2017;11:171. doi:10.3389/fnbeh.2017.00171

46. Won S, Ko JH, Jeon H, Park SS, Kim SN. Co-Administration of Gagam-Sipjeondaebo-Tang and Ibuprofen Alleviates the Inflammatory Response in MPTP-Induced Parkinson's Disease Mouse Model and RAW264.7 Macrophages. *Pathogens*. 2021;10(3):268. doi:10.3390/pathogens10030268

47. Wright JW, Harding JW. Contributions by the Brain Renin-Angiotensin System to Memory, Cognition, and Alzheimer's Disease. *J Alzheimers Dis*. 2019;67(2):469–480. doi:10.3233/JAD-181035

48. Kamath T, Abdulraouf A, Burris SJ, et al. Single-cell genomic profiling of human dopamine neurons identifies a population that selectively degenerates in Parkinson's disease. *Nat Neurosci*. 2022;25(5):588–595. doi:10.1038/s41593-022-01061-1

49. Jackson L, Eldahshan W, Fagan SC, Ergul A. Within the Brain: the Renin Angiotensin System. *Int J Mol Sci*. 2018;19(3):876. doi:10.3390/ijms19030876

50. Labandeira-Garcia JL, Valenzuela R, Costa-Besada MA, Villar-Cheda B, Rodriguez-Perez AI. The intracellular renin-angiotensin system: friend or foe. Some light from the dopaminergic neurons. *Prog Neurobiol*. 2021;199:101919. doi:10.1016/j.neurobio.2020.101919

51. Kim EA, Choi J, Han AR, et al. 2-Cyclopropylimino-3-methyl-1,3-thiazoline hydrochloride inhibits microglial activation by suppression of nuclear factor-kappa B and mitogen-activated protein kinase signaling. *J Neuroimmune Pharmacol*. 2014;9(4):461–467. doi:10.1007/s11481-014-9542-4

52. Wik JA, Skålhegg BS. T Cell Metabolism in Infection. *Front Immunol*. 2022;13:840610. doi:10.3389/fimmu.2022.840610

53. Meckiff BJ, Ramírez-Suástegui C, Fajardo V, et al. Imbalance of Regulatory and Cytotoxic SARS-CoV-2-Reactive CD4+ T Cells in COVID-19. *Cell*. 2020;183(5):1340–1353.e16. doi:10.1016/j.cell.2020.10.001

54. Rodriguez-Mogeda C, van Ansenwoude CMJ, van der Molen L, Strijbis EMM, Mebius RE, de Vries HE. The role of CD56bright NK cells in neurodegenerative disorders. *J Neuroinflam*. 2024;21(1):48. doi:10.1186/s12974-024-03040-8

55. Tsagkaris C, Bilal M, Aktar I, et al. Cytokine Storm and Neuropathological Alterations in Patients with Neurological Manifestations of COVID-19. *Curr Alzheimer Res*. 2022;19:641–657. doi:10.2174/1567205019666220908084559

56. Lauritsen J, Romero-Ramos M. The systemic immune response in Parkinson's disease: focus on the peripheral immune component. *Trends Neurosci*. 2023;46(10):863–878. doi:10.1016/j.tins.2023.07.005

57. Li Q, Wang Y, Sun Q, et al. Immune response in COVID-19: what is next? *Cell Death Differ*. 2022;29(6):1107–1122. doi:10.1038/s41418-022-01015-x

58. Supriya R, Gao Y, Gu Y, Baker JS. Role of Exercise Intensity on Th1/Th2 Immune Modulations During the COVID-19 Pandemic. *Front Immunol*. 2021;12:761382. doi:10.3389/fimmu.2021.761382

59. Yang J, Song H, Hao X. Whole-transcriptome sequencing data reveals a disparate cognitive and immune signature in COVID-19 patients with and without dementia. *J Med Virol*. 2023;95(1):e28177. doi:10.1002/jmv.28177

60. Perkins ND. Post-translational modifications regulating the activity and function of the nuclear factor kappa B pathway. *Oncogene*. 2006;25(51):6717–6730. doi:10.1038/sj.onc.1209937

61. Nihira K, Ando Y, Yamaguchi T, Kagami Y, Miki Y, Yoshida K. Pim-1 controls NF-kappaB signalling by stabilizing RelA/p65. *Cell Death Differ*. 2010;17(4):689–698. doi:10.1038/cdd.2009.174

62. Phani S, Loike JD, Przedborski S. Neurodegeneration and inflammation in Parkinson's disease. *Parkinsonism Relat Disord*. 2012;18:S207–S209. doi:10.1016/S1353-8020(11)70064-5

63. Schmitz ML, Kracht M, Saul VV. The intricate interplay between RNA viruses and NF-κB. *Biochim Biophys Acta*. 2014;1843(11):2754–2764. doi:10.1016/j.bbamcr.2014.08.004

64. Das G, Mukherjee N, Ghosh S. Neurological Insights of COVID-19 Pandemic. *ACS Chem Neurosci*. 2020;11(9):1206–1209. PMID: 32320211. doi:10.1021/acschemneuro.0c00201

65. Mankad K, Perry MD, Mirsky DM, Rossi A. COVID-19: a primer for Neuroradiologists. *Neuroradiology*. 2020;62(6):647–648. PMCID: PMC7186113. doi:10.1007/s00234-020-02437-5

66. Mao L, Jin H, Wang M, et al. Neurologic manifestations of hospitalized patients with Coronavirus Disease 2019 in Wuhan, China. *JAMA Neurol*. 2020;77(6):683–690. doi:10.1001/jamaneurol.2020.1127

67. Meyer PT, Hellwig S, Blazhenets G, Hosp JA. Molecular Imaging Findings on Acute and Long-Term Effects of COVID-19 on the Brain: A Systematic Review. *J Nucl Med*. 2022;63(7):971–980. doi:10.2967/jnumed.121.263085

68. Generoso JS, Barichello de Quevedo JL, Cattani M, et al. Neurobiology of COVID-19: how can the virus affect the brain? *Braz J Psychiatry*. 2021;43(6):650–664. doi:10.1590/1516-4446-2020-1488

69. Cimmino G, Conte S, Morello M, et al. Vitamin D Inhibits IL-6 Pro-Atherothrombotic Effects in Human Endothelial Cells: a Potential Mechanism for Protection against COVID-19 Infection? *J Cardiovasc Dev Dis*. 2022;9(1):27. doi:10.3390/jcdd9010027

70. Li N, Wang JX, Huo TT, Zhao JR, Wang TJ. Associations of IL-1β and IL-6 gene polymorphisms with Parkinson's disease. *Eur Rev Med Pharmacol Sci*. 2021;25(2):890–897. doi:10.26355/eurrev_202101_24657

71. Brundin P, Nath A, Beckham JD. Is COVID-19 a Perfect Storm for Parkinson's Disease? *Trends Neurosci*. 2020;43(12):931–933. PMID: 33158605; PMCID: PMC7577682. doi:10.1016/j.tins.2020.10.009

72. Matschke J, Lütgehetmann M, Hagel C, et al. Neuropathology of patients with COVID-19 in Germany: a post-mortem case series. *Lancet Neurol*. 2020;19(11):919–929. doi:10.1016/S1474-4422(20)30308-2

73. Braak H, Del Tredici K, Rüb U, de Vos RA, Jansen Steur EN, Braak E. Staging of brain pathology related to sporadic Parkinson's disease. *Neurobiol Aging*. 2003;24(2):197–211. doi:10.1016/s0197-4580(02)00065-9

74. Dickson DW. Neuropathology of Parkinson disease. *Parkinsonism Relat Disord*. 2018;1(Suppl 1):S30–S33. doi:10.1016/j.parkreldis.2017.07.033

75. McQuaid C, Brady M, Deane R. SARS-CoV-2: is there neuroinvasion? *Fluids Barriers CNS*. 2021;18(1):32. doi:10.1186/s12987-021-00267-y

76. Medina-Enríquez MM, Lopez-León S, Carlos-Escalante JA, Aponte-Torres Z, Cuapio A, Wegman-Ostrosky T. ACE2: the molecular doorway to SARS-CoV-2. *Cell Biosci*. 2020;10(1):148. doi:10.1186/s13578-020-00519-8

77. Urmila A, Rashmi P, Nilam G, Subhash B, Li X. Recent Advances in the endogenous brain renin-angiotensin system and drugs acting on It. *J Renin Angiotensin Aldos Syst*. 2021;9293553. doi:10.1155/2021/9293553

78. Xia H, Lazartigues E. Angiotensin-converting enzyme 2 in the brain: properties and future directions. *J Neurochem*. 2008;107(6):1482–1494. PMID: 19014390; PMCID: PMC2667944. doi:10.1111/j.1471-4159.2008.05723.x

79. Morganstein T, Haidar Z, Trivlidis J, et al. Involvement of the ACE2/Ang-(1-7)/MasR Axis in Pulmonary Fibrosis: implications for COVID-19. *Int J Mol Sci*. 2021;22(23):12955. doi:10.3390/ijms222312955

80. Haddadi K, Ghasemian R, Shafizad M. Basal Ganglia Involvement and altered mental status: a unique neurological manifestation of Coronavirus Disease 2019. *Cureus*. 2020;12(4):e7869. doi:10.7759/cureus.7869